



FORTH

INSTITUTE OF MOLECULAR BIOLOGY & BIOTECHNOLOGY



Studies of transcription factors contributing to *Drosophila* early neurogenesis

Master thesis
2021

Master program: Molecular Biology and Biomedicine

Student: Margarita Dimitra Masoura

Advisor: Prof. Delidakis Christos

Laboratory of developmental genetics, IMBB-FORTH

To Mythra and Pontsi.

Contents

Abstract	1
Περίληψη.....	2
1. Introduction.....	4
1.1 <i>Drosophila melanogaster</i> as a model system for developmental neurobiology.....	4
1.2 Development of the central nervous system (CNS) in the fruit fly	4
1.2.1 Modes of neuroblast proliferation	5
1.3 Development of the embryonic CNS	6
1.3.1 Spatiotemporal cues give embryonic neuroblasts unique identities.....	6
1.3.2 Notch-mediated lateral inhibition as a driver of neuroblast selection in the neuroectoderm.....	8
.....	9
1.4 Crucial players of embryonic neurogenesis	9
1.4.1 Proneural genes and daughterless (da).....	10
1.4.2 E(spl) genes.....	11
1.4.3 Mechanisms of E(spl) mediated repression of proneural targets	11
1.5 Mutations in proneural, da and E(spl) genes result in impaired CNS development	12
1.5.1 Proneural and da gene deletions leads to neural hypoplasia	12
1.5.2 E(spl) genes deletions lead to excessive neural hyperplasia	14
1.6 Aim of the study.....	15
2. Materials and Methods.....	17
2.1 Fly stocks and crosses	17
2.2 Immunostaining	18
2.3 Embryo fixation for cHIP	19
2.4 Nuclear extraction.....	19
2.5 Chromatin pull down and sequencing.....	20
2.6 Western blot.....	21
2.7 Quantitative PCR (qPCR)	21
3. Results.....	22
3.1 AS-C and E(spl) gene deletions lead to delayed Dpn expression and excessive neuroblast generation.	22
3.1.1 Neuroblasts are formed by the stage 8 in double mutants.....	22
3.1.2 Excessive generation of Dpn-negative neuroblasts in double mutants of stage 9.....	24
3.1.3 Embryonic stage 10 is marked by massive rebound of Dpn expression and a burst of neuroblast formation in double mutants.....	25
3.1.4 Neurogenic phenotypes of double mutants at 12-13 developmental stages.....	26

3.2 Biotin pull-down and DNA sequencing to identify Daughterless' binding sites.	27
3.2.1 Selection of Gal4 driver to promote the expression in the neuroectoderm	27
3.2.2 Daughterless pull-down assays.	27
4. Discussion	35
4.1 Proneurals and E(spl) promote its defects independently	35
4.2 The role of dpn in embryonic neuroblasts	35
4.3 Understanding the role of Da in embryonic neurogenesis	36
4.4 Technical improvement of our protocol will provide robustness in our pull-down method. ..	37
5. Bibliography	38

Abstract

Development of the central nervous system constitutes a highly complex process that requires precise spatiotemporal regulation. In *Drosophila melanogaster*, neurogenesis initiates at the embryo and continues until pupal stages. Embryonic neurogenesis begins at the stage 8 with the generation of neural progenitors, called neuroblasts. Neuroblasts derive from the ventral ectoderm and are specified through the process of Notch-mediated lateral inhibition. During this process, effectors of Notch pathway, called Enhancer of split E(spl) and the proneural genes are antagonizing, creating an intercellular feedback loop. As a result, specific neuroectodermal cells are singled out and induce the neural fate. Upon its generation, neuroblasts delaminate from the ectodermal sheet and undergo multiple rounds of asymmetrical divisions to self-renew and give rise to a ganglion mother cell (GMC). GMC divides once again, forming a pair of neurons and/or glia. Even though mechanisms implicated in lateral inhibition have been extensively studied, the complex interplay between proneural genes and Notch is yet to be fully resolved. Proneural genes encode bHLH transcriptional activators which heterodimerize with another bHLH factor, called Daughterless (Da), to promote induction of the neural fate. On the other hand, genes of the E(spl) locus encode bHLH transcriptional repressors that downregulate proneural activity and lead to epidermal specification. Mutations in E(spl) result in the development of neural hyperplasia. Whereas, absence of proneural genes leads to the partial loss of neuroblasts, accounting for 20-25%. Neuroblasts that manage to be formed exhibit a temporary pause of its divisions and lack expression of certain genes including deadpan (dnp). Divisions and dnp expression restart in later embryonic stages. The mechanisms implicated in this “stalled state” are yet to be uncovered. To better understand this process, we studied embryos lacking both proneurals and E(spl) genes referred as “double mutants”. We observe a hyperplastic phenotype with temporary arrest of neuroblast divisions and delayed dnp expression. We also studied the role of Da in the neuroectoderm. While mutations on either da or proneurals cause only a partial loss of neuroblasts, embryos lacking both are aneural. We wanted to examine if Da can activate distinct gene targets in the neuroectoderm in a proneural independent manner. Thus, we developed a CHIP-sequencing protocol to identify Da targets. Our technique is based on a biotin pull-down strategy for the precipitation of Da. We didn't identify unique neural targets. However, we validated the efficiency of our protocol, which needs further optimization.

Περίληψη

Η ανάπτυξη του κεντρικού νευρικού συστήματος αποτελεί μια από τις πιο σύνθετες βιολογικές διεργασίες και απαιτεί ακριβή γονιδιακή ρύθμιση στο χώρο και στο χρόνο. Στη *Drosophila melanogaster*, η διαδικασία της νευρογένεσης εκκινεί κατά τα εμβρυικά στάδια και συνεχίζεται μέχρι το σχηματισμό της νύμφης. Η εμβρυϊκή νευρογένεση ξεκινά στο στάδιο 8 με τη δημιουργία πρόδρομων νευρικών κυττάρων, που ονομάζονται νευροβλάστες. Τα κύτταρα αυτά προέρχονται από την περιοχή του κοιλιακού εκτοδέρματος. Η επιλογή των κυττάρων που θα επάγουν τη νευρική τύχη επιτυγχάνεται μέσω της διαδικασίας της πλευρικής αναστολής. Συγκεκριμένα, οι Enhancer of split E(spl), οι οποίοι αποτελούν άμεσους γονιδιακούς στόχους του Notch μονοπατιού και οι προνευρικοί παράγοντες ανταγωνίζονται μεταξύ τους, δημιουργώντας μία δια κυτταρική λούπα ανατροφοδότησης. Ως επακόλουθο, συγκεκριμένα νευροεκτοδερμικά κύτταρα επιλέγονται για να ακολουθήσουν τη νευρική τύχη και διαφοροποιούνται σε νευροβλάστες. Κατά τη δημιουργία τους, οι νευροβλάστες αποκολλώνται από τη στιβάδα του εκτοδέρματος προς το εσωτερικό, όπου διαιρούνται ασύμμετρα, δίνοντας γένεση σε ένα νέο νευροβλάστη και ένα ganglion mother cell (GMC). Το GMC διαιρείται με τη σειρά του, σχηματίζοντας ένα ζευγάρι νευρώνων και / ή γλιακών κυττάρων. Παρά το γεγονός ότι οι μοριακοί μηχανισμοί που διέπουν την πλευρική αναστολή έχουν μελετηθεί εκτενώς, η πολυπλοκότητα της σχέσης των προνευρικών γονιδίων και του Notch μονοπατιού δεν έχει διασαφηνιστεί πλήρως. Τα προνευρικά γονίδια κωδικοποιούν bHLH μεταγραφικούς ενεργοποιητές, οι οποίοι ετεροδιμερίζονται με έναν άλλο bHLH παράγοντα, το Daughterless (Da). Το διμερές σύμπλοκο προάγει την επαγωγή νευρικών γονιδίων. Σε αντιδιαστολή, τα γονίδια του γενετικού τύπου E(spl) κωδικοποιούν bHLH μεταγραφικούς καταστολείς, οι οποίοι αναστέλλουν τα προνευρικά γονίδια και οδηγούν σε επιδερμική διαφοροποίηση. Απώλεια λειτουργίας των E(spl) γονιδίων έχει ως αποτέλεσμα την ανάπτυξη νευρικής υπερπλασίας, ενώ η απουσία των προνευρικών γονιδίων οδηγεί στη μερική απώλεια νευροβλαστών, της τάξης του 20-25%. Οι νευροβλάστες που καταφέρνουν να σχηματιστούν εμφανίζουν μια παρωδική παύση των κυτταρικών διαιρέσεων, καθώς επίσης αδυνατούν να εκφράσουν ορισμένα γονίδια συμπεριλαμβανομένου του *deadpan* (*dpr*). Οι διαιρέσεις και η έκφραση του *dpr* επανεκκινούν σε μεταγενέστερα εμβρυικά στάδια. Οι μηχανισμοί που ευθύνονται για αυτή την προσωρινή παύση παραμένουν άγνωστοι. Στην προσπάθεια να κατανοήσουμε καλύτερα αυτήν τη διαδικασία, μελετήσαμε έμβρυα, στα οποία απουσιάζουν ταυτόχρονα τα προνευρικά και τα γονίδια του E(spl) γονιδιακού τύπου και αναφέρονται ως «διπλά μεταλλάγματα». Παρατηρούμε έναν υπερπλασία του νευρικού συστήματος με προσωρινή διακοπή στις διαιρέσεις των νευροβλαστών καθώς και καθυστερημένη έκφραση του *dpr*. Επιπλέον, μελετήσαμε το ρόλο του Da στο νευροεκτόδερμα. Ενώ οι επιμέρους μεταλλάξεις

στο da ή στα προνευρικά γονίδια προκαλούν μόνο μερική απώλεια νευροβλαστών, τα έμβρυα που στερούνται και των δύο αδυνατούν να αναπτύξουν νευρικό σύστημα. Δεδομένων των παραπάνω, εξετάσαμε αν το Da μπορεί να ενεργοποιήσει γονιδιακούς στόχους στο νευροεκτόδερμα, ξεχωριστούς από τους στόχους των προνευρικών παραγόντων. Για το σκοπό αυτό, αναπτύξαμε ένα πρωτόκολλο κατακρήμνισης χρωματίνης σε συνδυασμό με αλληλούχιση του DNA για τον προσδιορισμό των στόχων του Da. Η τεχνική κατακρήμνισης του Da βασίζεται στο σύστημα βιοτίνης-στρεπταβιδίνης. Δεν εντοπίσαμε μοναδικούς νευρικούς στόχους. Ωστόσο, επιβεβαιώσαμε την αποτελεσματικότητα του πρωτοκόλλου μας, το οποίο χρειάζεται περαιτέρω βελτιστοποίηση.

1. Introduction

1.1 *Drosophila melanogaster* as a model system for developmental neurobiology

The mechanisms implicated in the nervous system development have always been an intriguing enigma, with many questions remaining unanswered or even unaddressed until today. The difficulty in dissecting the insights governing neurogenesis lies in the perplexed and multi scaled interactions among the factors participating in those processes, as well as the rapidly alternating temporal events. Unraveling the intricacies contributing to the formation and cellular diversity of the nervous system is considered one of the major challenges in developmental biology.

In order to shed light to the molecular trajectories shaping the neural development, the scientific community focused on the study of *Drosophila melanogaster*. The fruit fly provides a low-cost and time-saving platform, enabling scientists to pose multiple biological questions. Having already been established as a powerful model for genetic research -for more than a century- it continues serving as a state-of-the-art organism for the study of many other biological aspects.

The discovery of genes, implicated in the *Drosophila* embryo development and the elucidation of developmental signaling networks paved the way for a new era in *Drosophila* research ¹. Identification of homologous counterparts and analogous developmental pathways in vertebrates further underlined its role as a prevalent model organism. Along with the advent of striking molecular and imaging tools, the effort to uncover the intricacies of development has been intensified in many fields, including the developmental neurobiology. The study of neural stem cells in the fruit fly, has critically added to our understanding on how such a great cellular diversity is attained in the nervous system ².

1.2 Development of the central nervous system (CNS) in the fruit fly

In *Drosophila*, development of the CNS occurs in distinct developmental stages. Initiating at the embryos, neurogenesis continues in the larvae and terminates at pupal stages (Figure 1A). Though, this theory is still debated, as there is emerging evidence of adult neurogenesis upon injury and damage ^{3,4}. Neuroblasts, which constitute the neural progenitors of the fruit fly divide in a stem cell like manner to generate neural and glial cells.

Embryonic neuroblasts are responsible for the production of almost all neurons and glia observed in the larval CNS ⁵. However, in adult flies only 10% of neural and glial cells represent embryonic derived lineages ⁶. Upon completion of their divisions, embryonic neuroblasts are either wiped out through apoptosis, or enter a quiescent state, pausing its proliferation. Reboot of cell divisions is accomplished in larval stages, whereby neuroblasts restart its propagation giving rise to the rest 90% of the adult CNS ⁷. By the end of pupal stages and soon before fly enclose, all neuroblasts are eliminated, either due to programmed cell death or because of cell cycle exit.

1.2.1 Modes of neuroblast proliferation

According to its daughter cell proliferation profiles neuroblasts are classified into three distinct types of (Type 0, Type I, Type II) ⁸ (Figure 1B). Type 0 neuroblasts divide symmetrically to self-renew and directly generate a neuron. Type I neuroblasts follow a program of asymmetrical divisions, leading to the production of another neuroblast and a ganglion mother cell (GMC). GMC divides once, forming neurons and glial cells. Finally, Type II neuroblasts amplify its progeny by the generation of intermediate progenitors (INPs). INPs self-renew and produce GMCs, which subsequently give rise to neurons and glia.

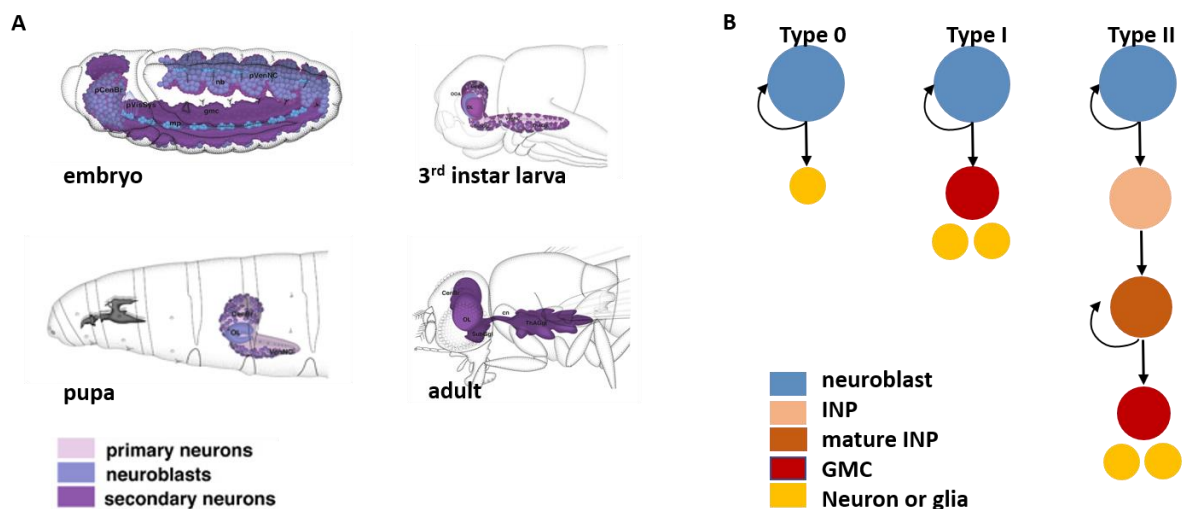


Figure 1 (A) Schematic representation of the central nervous system during embryonic, larval, pupal and adult stages in *Drosophila melanogaster* (Adapted from *Atlas of Drosophila Development* by Volker Hartenstein published by Cold Spring Harbor Laboratory Press, 1993). (B) Types of neuroblast divisions. Type 0 divide once, regenerating themselves and producing a neuron. Type I neuroblasts divide asymmetrically. Type II neuroblasts generate an intermediate progenitor (INP). INP proceeds to asymmetrical division to self-renew and produce a ganglion mother cell (GMC).

1.3 Development of the embryonic CNS

By the onset of the 20th century, studies in the peripheral nervous system of *Drosophila melanogaster* led to the identification of proneural genes, which act as the major neural determinants. In brief, it was observed that upon loss of proneural genes, bristles, which constitute sensory organs of adult flies fail to form^{9,10}. Few decades later it was revealed that proneural genes are closely located inside the genome and form a complex, referred as the Achaete-Scute complex (AS-C)¹¹. These genes were also found to be key regulators of the CNS. Parallel studies, focusing on the development of the peripheral and central nervous system have provided significant insights into how nervous system is generated in the fruit fly.

Embryonic neurogenesis begins at the stage 8, approximately 3 hours after egg laying and shortly after gastrulation. Neuroblasts arise from a region of the ventral ectoderm, called neuroectoderm, in five successive waves (Figure 3A). Upon its generation, neuroblasts delaminate from the ectodermal sheet¹² (Figure 3B) and undergo repeated Type I divisions, renewing themselves and budding off smaller GMCs. GMCs divide once to give rise to a pair of neurons and/or glial cells (Figure 3C).

1.3.1 Spatiotemporal cues give embryonic neuroblasts unique identities

Embryonic CNS consists of the brain and the ventral nerve chord (VNC). Unlike the perplexed structure of the developing brain, embryonic VNC provides a simpler platform for understanding the early neurogenesis events and it has been extensively studied. It consists of repeated hemi segments, that are generated bilaterally and separated by the midline. 30 neuroblasts arise in each hemi-segment in a stereotypical spatial pattern¹³ (Figure 2A). Precise positional information enables neuroblasts of each hemi-segment to develop unique properties. These spatial signals arise from the prepatterned structure of the neuroectoderm, along the anterior-posterior (A-P) and the dorsal ventral (D-V) axis¹⁴. A-P axis is initially specified by the expression of maternal, gap and pair rule genes, which in turn promote the expression of segment polarity genes in tightly restricted bands, leading to the formation of distinct neuroectodermal rows¹⁵. Along D-V axis, a set of three genes, termed columnar genes, is responsible for the generation of precisely defined columns. Expression of columnar genes is crucial for shaping neuroblast identity, within each column¹⁶⁻¹⁸. Overall, subdivision

of neuroectoderm in the two axes, creates a grid, that contains multiple neural equivalence groups. Each group receives an exclusive set of positional cues, leading neuroblasts, to the acquisition of unique insights ¹⁴.

Apart from the spatial cues, neuroblasts also receive multiple temporal stimuli, allowing them to generate multiple types of progeny and thus providing a greater pool of neuronal diversity. This is attained by the sequential expression of specific transcription factors, referred as “Temporal Transcription Factors (TTFs)” ^{19,20}. The temporal cascade includes the serial activation of five main genes: Hunchback (Hb), Kruppel (Kr), Pdm, Castor (Cas) and Grainyhead (Gh) (Figure 2B). Each TTF promotes the induction of the next gene in line, enabling the proper transition across temporal windows. For example, Hb which is the first factor expressed,

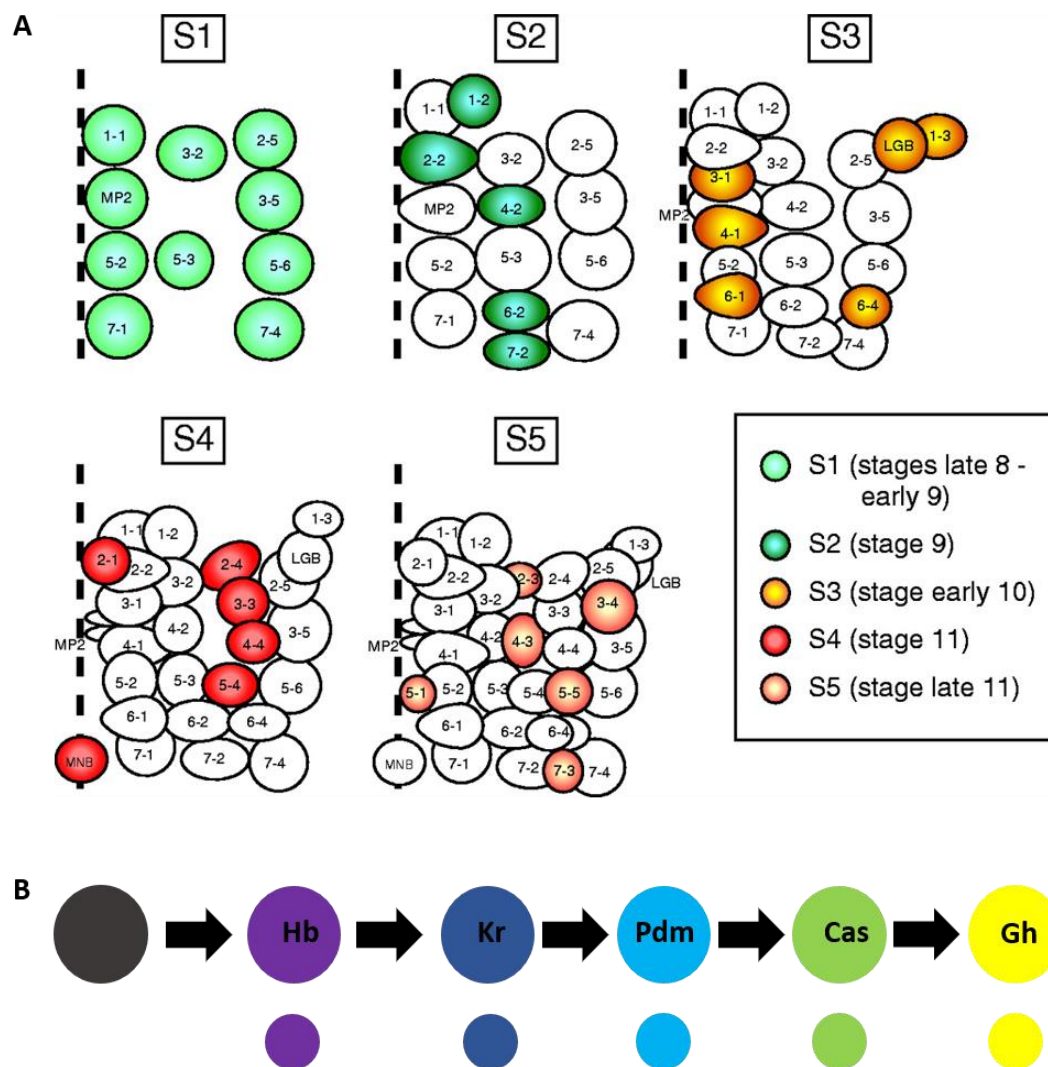


Figure 2 Neuroblasts and its progeny bear unique identities, shaped in space and time. (A) Schematic representation of a typical hemi-segment across the five waves of neuroblast generation. Patterning of the neuroectoderm along A-P and D-V axis leads to the generation of neuroblasts in a stereotyped spatial manner. 30 neuroblasts are created in each hemi-segment and are organized in seven rows and three columns. (B) Demonstration of the TTFs participating in the sequential temporal cascades. Each factor is expressed in distinct time window, providing neuroblast and its progeny unique identities.

activates its successor, Kr and is being downregulated. Thus, neuroblasts and its daughter cells are specified according to its birth order. This process ensures that GMCs born at different time windows acquire distinct fates and subsequently give rise in multiple types of neurons and glia.

1.3.2 Notch-mediated lateral inhibition as a driver of neuroblast selection in the neuroectoderm

Neuroectodermal cells have the potential to initiate two distinct transcriptional programs, leading either to the acquisition of the neural fate or to the generation of epidermal progenitors ^{21,22}. Cell fate specification is achieved by Notch-mediated lateral inhibition, a process emerging in multiple developmental contexts to determine binary cell fate choices ²³. In neuroectoderm, genes of the AS-C and effectors of the Notch pathway constitute the key contributors of neural and epidermal cell fate respectively ²².

According to the classic model of lateral inhibition, presented in Figure 3D, interactions between proneural factors and Notch downstream targets lead to the generation of an intercellular feedback loop. While Notch receptor is uniformly expressed, proneural factors are detected in groups of neuroectodermal cells, termed “proneural clusters”. Induction of the AS-C genes leads to the upregulation of the transmembrane protein Delta, which act as a ligand of the Notch receptor. Dose-dependent activation of Delta by proneurals plays key role in the process of lateral inhibition ²⁴. Once extracellular domain of Delta interacts with the concomitant domain of Notch receptor, serial proteolytic cleavages of the latter, result in the release of Notch intracellular domain (NICD). NICD is transferred into the nucleus and together with Suppressor of Hairless and Mastermind promote the expression of gene targets ^{25,26}. The outcome of Notch signaling in the neighboring cells is the induction of the genes of the Enhancer of split locus (E(spl)). E(spl) proteins are transcriptional repressors, which downregulate proneural gene activity. Finally, all but one cells of each proneural cluster are eliminated from neural fate and acquire the epidermal one. The single cell that manages to maintain proneural activity becomes the neural progenitor.

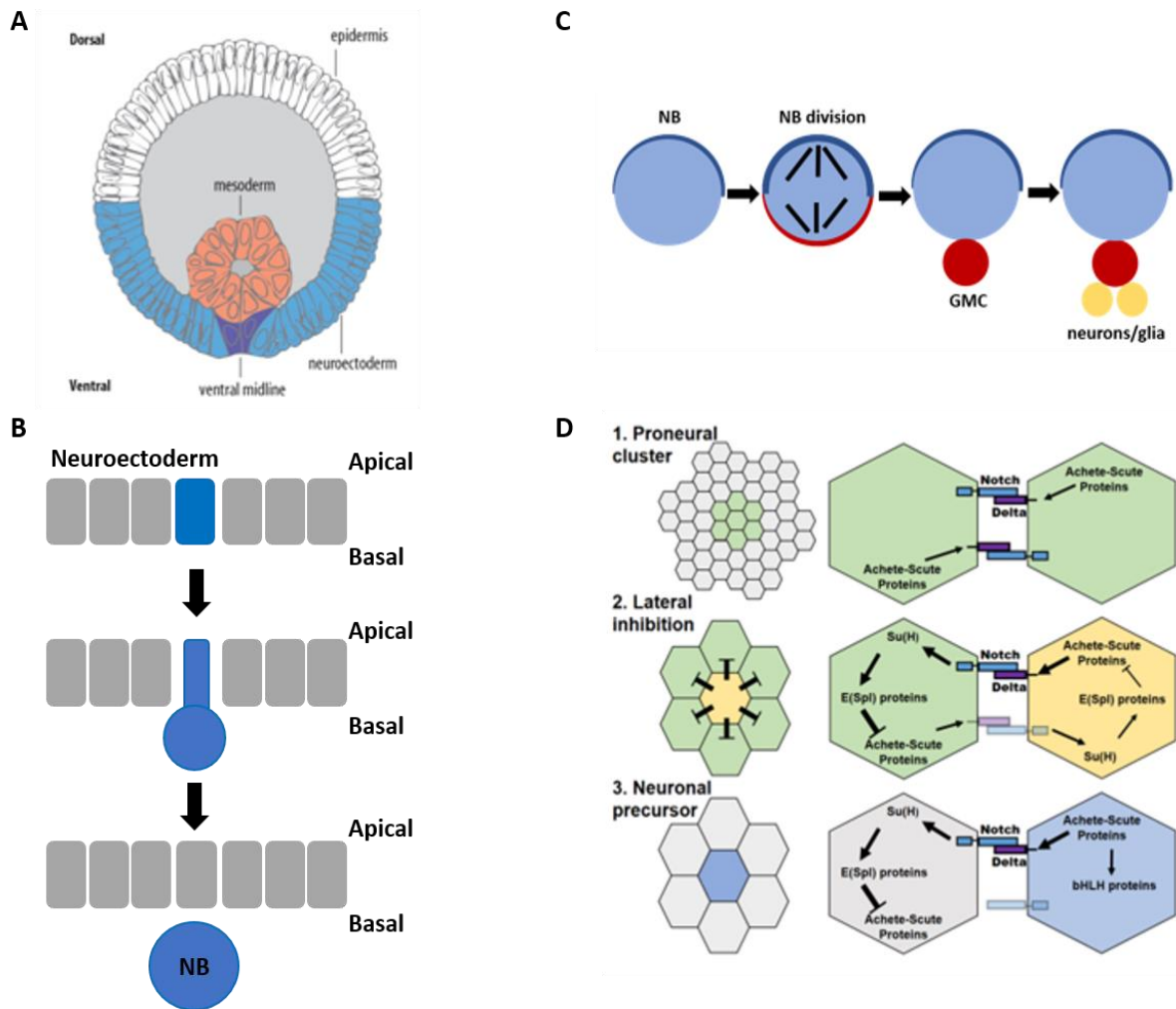


Figure 3 Embryonic neurogenesis in *Drosophila melanogaster*. (A) Dorsoventral pattern of the embryo. Neuroblasts arise from the ventral ectoderm, called neuroectoderm (blue region). Mesoderm (pink) has already been formed (Adapted from *Atlas of Drosophila Development* by Volker Hartenstein published by Cold Spring Harbor Laboratory Press, 1993). (B) Delamination of neuroblasts from neuroectoderm and internalization to the basal side of the embryo. (C) Neuroblast asymmetrical divisions. Neuroblast division results in the generation of another neuroblast (blue) and a GMC (red). GMCs divide once to give rise to a pair of neurons and/ or glial cells (yellow). (D) Notch mediated lateral inhibition drives the epidermal/neural cell specification. Groups of cells expressing the proneural genes are highlighted with green. Delta is induced in cells of the proneural cluster. Notch – Delta interaction leads to the activation of Notch signaling in the neighboring cells, which in turn promotes the *E(spl)* gene expression. *E(spl)* repress proneural activity. Only one cell, that expresses genes of the AS-C at high levels retains neural potential and becomes neuroblast. This cell does not receive Notch signaling (Picture adapted by http://www.mun.ca/biology/desmid/brian/BIOL3530/DEVO_12/devo_12.html).

1.4 Crucial players of embryonic neurogenesis

The process of lateral inhibition drives the specification in neuroectoderm, enabling the selection of cells that acquire the neural fate. Even though a great progress has been made in the proneural-*E(spl)* interplay, the emerging multi-scaled interactions are yet to be fully uncovered. Genes of both complexes as well as their interactors continue being in the

spotlight of scientific research. A detailed description of our current knowledge about these genes and its products is presented in the following paragraphs.

1.4.1 Proneural genes and daughterless (da)

The AS-C is located in the X chromosome of the fruit fly and consists of a set of 4 genes, namely achaete (ac), scute (sc), lethal of scute (l'sc) and asense (ase)^{27,28}. Unlike ac, sc, and l'sc, which act in the neuroectoderm, ase is expressed in later stages of embryonic development. It has been shown that these genes are expressed in a tissue specific manner and act as promoters of neural specification^{9,10}. In addition to the genes of the AS-C, three more genes have later been identified to confer proneural activity [atonal (ato), cousin of atonal (cato) and absent MD neurons and olfactory sensilla (amos)], constituting a second family of proneural genes in *Drosophila*²⁹⁻³¹. These gene family is mostly implicated in the formation of the peripheral nervous system (PNS). Homologous counterparts of both families have been discovered in vertebrates, also serving as positive regulators of the neurogenic program³². Within the proneural clusters, proneural genes are activated by the columnar genes³³.

All four genes of the AS-C share sequence similarity with each other and with daughterless (da), a gene implicated in the sex determination^{34,35}. da is located at the second chromosome of *Drosophila* and plays vital roles in multiple developmental contexts. In early embryos, Da is of maternal origin and is mainly implicated in the sex determination, while in later stages zygotic product is expressed, contributing to the nervous system development³⁶. Unlike proneural restricted expression pattern, da is activated ubiquitously³⁷.

Genes of the AS-C as well as da encode transcriptional factors that contain a basic helix loop helix (bHLH) domain. bHLH constitutes a structural motif that enables DNA binding and dimerization (Figure 4)³⁸. Through their bHLH domains, proneural factors form heterodimers with Daughterless (Da) and bind to DNA, leading to the activation of neurogenic genes. Proneural-Da heterodimer generation is antagonized by the action of extramacrochaetae (emc). emc produces an HLH protein that lacks the ability of binding to DNA sequences³⁹. It inhibits proneural activity through the sequestration of either proneural proteins or Da. Thus, formation of functionable heterodimers is prevented and proneural gene target expression is abolished.

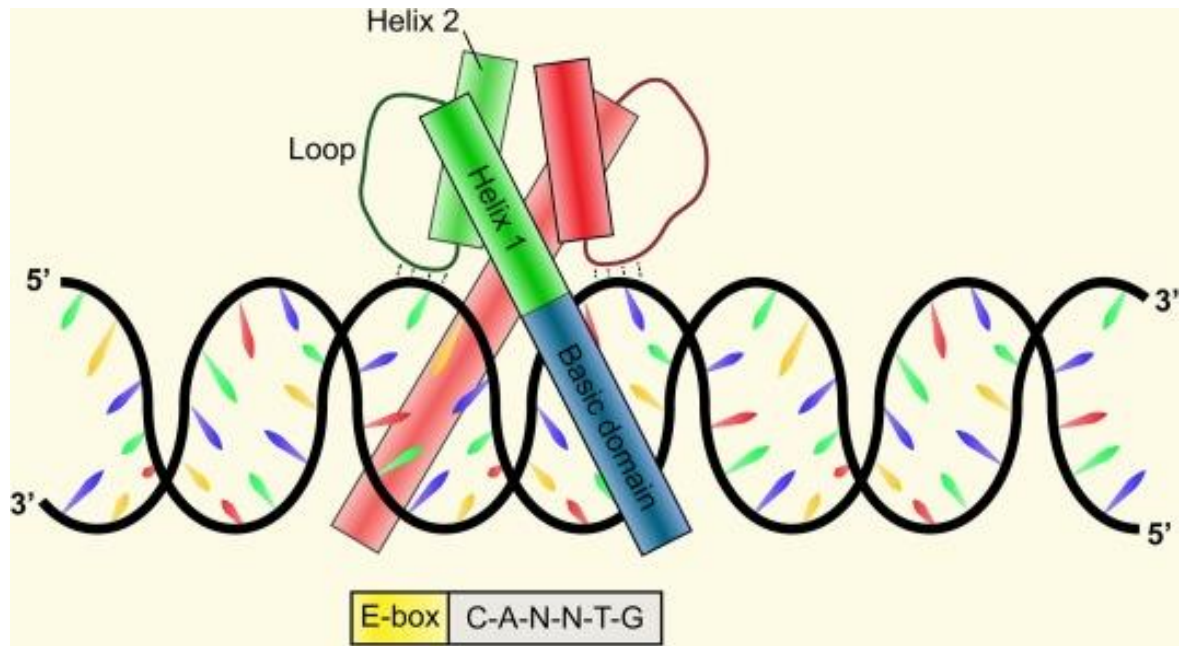


Figure 4 Schematic representation of basic helix loop helix (bHLH) structural motif. BHLH consist of two α helices connected by a short loop. bHLH enable DNA binding and heterodimerization. bHLH recognize a consensus DNA sequence termed E-box. (Picture adapted by Dennis, Han, and Schuurmans 2019)

1.4.2 E(spl) genes

Besides Emc-mediated inhibitory effects on proneural activity, E(spl) proteins are also acting as prominent repressors of proneural genes, during the process of lateral inhibition. E(spl) gene complex lies in the third chromosome of the fruit fly and is comprised of 12 genes. All but one genes of the complex are activated upon response to Notch signaling⁴⁰. The largest gene class within the complex accounts for seven genes, which encode bHLH transcriptional factors [HLHmb, HLHmg, HLHmd, HLHm3, HLHm5, HLHm7, and E(spl)]^{41,42}. It is suggested that its activity is at least partially redundant during embryonic neurogenesis. Unlike proneural, these genes also contain an Orange domain, which enable them to act as repressors⁴³.

1.4.3 Mechanisms of E(spl) mediated repression of proneural targets

E(spl) genes of the HLH class are able to homo or heterodimerize through its bHLH motifs. Moreover, a subset of them forms dimers with Ac, Sc and Da, leading to the downregulation of proneural targets. Thus, one mechanism of proneural repression is its sequestration and the prevention of binding to its targets⁴⁴. A second way proposed to eliminate proneural

activity is the recruitment of E(spl) proteins onto the proneural-dependent enhancers and its interaction with the proneural-Da dimer. Interestingly, it has been suggested that this mechanism is able to function either upon E(spl) DNA binding or in an HLH independent manner ⁴⁵. For the latter mode of repression, E(spl) proteins interact with the C-terminal domain of Sc, which has been found to act also as a transactivation domain ⁴⁶. Nevertheless, proneural proteins manage to maintain its competence, within the proneural clusters. This is achieved through the generation of an autoregulatory feedback loop, giving the potential to one cell of the cluster to preserve high proneural expression levels and subsequently become neuroblast.

1.5 Mutations in proneural, da and E(spl) genes result in impaired CNS development

The prominent role of proneural, da and E(spl) genes in neurogenesis have been identified through a series of loss of function experiments. These studies led to the suggestion that genes of the AS-C are necessary and sufficient to promote induction of the neural fate. Moreover, it was shown that Da is also important for the initiation of embryonic neurogenesis. Though, its role is confined as the proneural major interactor and it is not able to confer proneural activity. Similar studies of the 80s and 90s have also underlined the importance of E(spl) genes in the process of lateral inhibition. First it has been identified that these genes constitute a part of Notch signaling network. Subsequently it was revealed that its repressive capacities lead to the promotion of epidermal fate at the expense of neural one.

1.5.1 Proneural and da gene deletions leads to neural hypoplasia

The effort to understand the role of proneural genes, initiated by studies of the peripheral nervous system (PNS) ¹⁰. Later it was revealed that similar processes also shape the generation of the CNS ²¹. Deletion of the genes of the AS-C causes lethality at the embryonic stages. Upon loss of the whole complex, proneural activity is completely eliminated in the PNS. On the contrary, within the CNS proneural activity is somehow retained even in the absence of those genes. Particularly, it is detected a decline in the number of delaminating neuroblasts, accounting for 20-25 % of total neuroblasts ⁴⁷. Neuroblasts that manage to be

formed present defective proliferation. Increased cell death is also observed on their progeny, at later stages ⁴⁷.

In a recent unpublished work conducted in our laboratory, loss of AS-C genes was studied in great detail, during distinct embryonic stages. It was revealed that the absence of these genes leads to a temporary pause of neuroblasts divisions, between embryonic stages 8-10. Moreover, expression of certain neuroblast-specific genes has also been abolished during these stages. Among those genes, deadpan (*dpn*) is included (Figure 5B). *dpn* encodes a bHLH transcriptional repressor ⁴⁸ and it is widely used as a molecular marker for neuroblast identification. By the end of the stage 10 and the early onset of stage 11 cell proliferation restarts and *dpn* expression is being restored within the neuroblasts (Figure 5B). However, this rebooting in cellular propagation is not able to rescue the severe defects, caused by the deletion. At later stages, it is observed severe impairment of the neuronal axon development and massive cell death, as previously described.

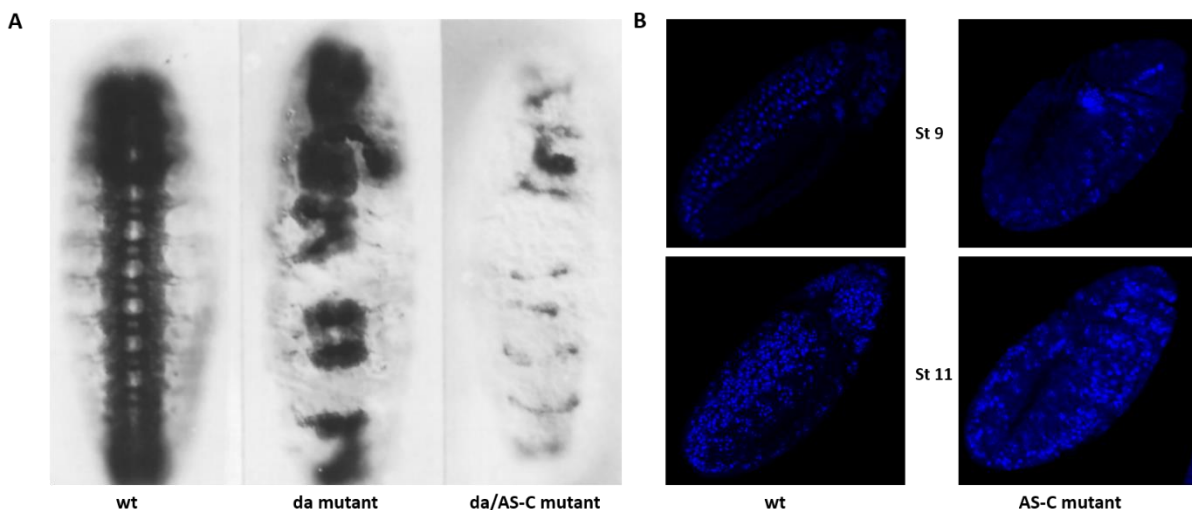


Figure 5 Mutations of *da* and proneurals lead to the defective nervous system development (A) Deletion of *da* results in impaired CNS structure. In the absence of both *da* and proneural genes, embryos are aneural (Adapted from Fernando Jiménez and Campos-Ortega 1990). (B) Neuroblasts in wt (left) and AS-C deficient (right) embryos. Neuroblasts are marked with *dpn*. At stage 9 (up) AS-C mutant embryos lack *dpn* expression. It is restored by the onset of stage 11.

da loss of function experiments demonstrates similar phenotypes to those observed in proneural deficiency (Figure 5A). Upon absence of *da*, all sensory neurons of the PNS fail to form, while defects are also detected in the CNS ^{49,50}. In a study examining the roles of proneurals and *da* in the CNS formation, Jimenez and Campos-Ortega discovered that the double deletion of *da* and proneural genes led to the complete loss of neuroblasts, resulting in aneural embryos ⁴⁷ (Figure 5A).

1.5.2 E(spl) genes deletions lead to excessive neural hyperplasia

Akin to the study of proneural genes, elucidation of the role of the E(spl) genes was accomplished through the examination of mutant embryonic phenotypes. Complete deletion of the locus is lethal at embryonic stages. In the absence of the complex, a severe neural hyperplasia emerges in the CNS ⁴¹, similar to that observed in Notch deficiencies (Figure 6). This suggests that E(spl) genes constitute the major Notch effectors implicated in the cell fate selection in neuroectoderm. Excessive neuroblast generation and therefore development of neural hypertrophy in E(spl) mutants is caused due to defects in the process of lateral inhibition. In particular, absence of these genes results in the expansion of proneural activity in neuroectodermal cells. Thus, neural fate is induced in more than one cells of each proneural cluster, finally leading to the production of supernumerary neuroblasts (Figure 6).

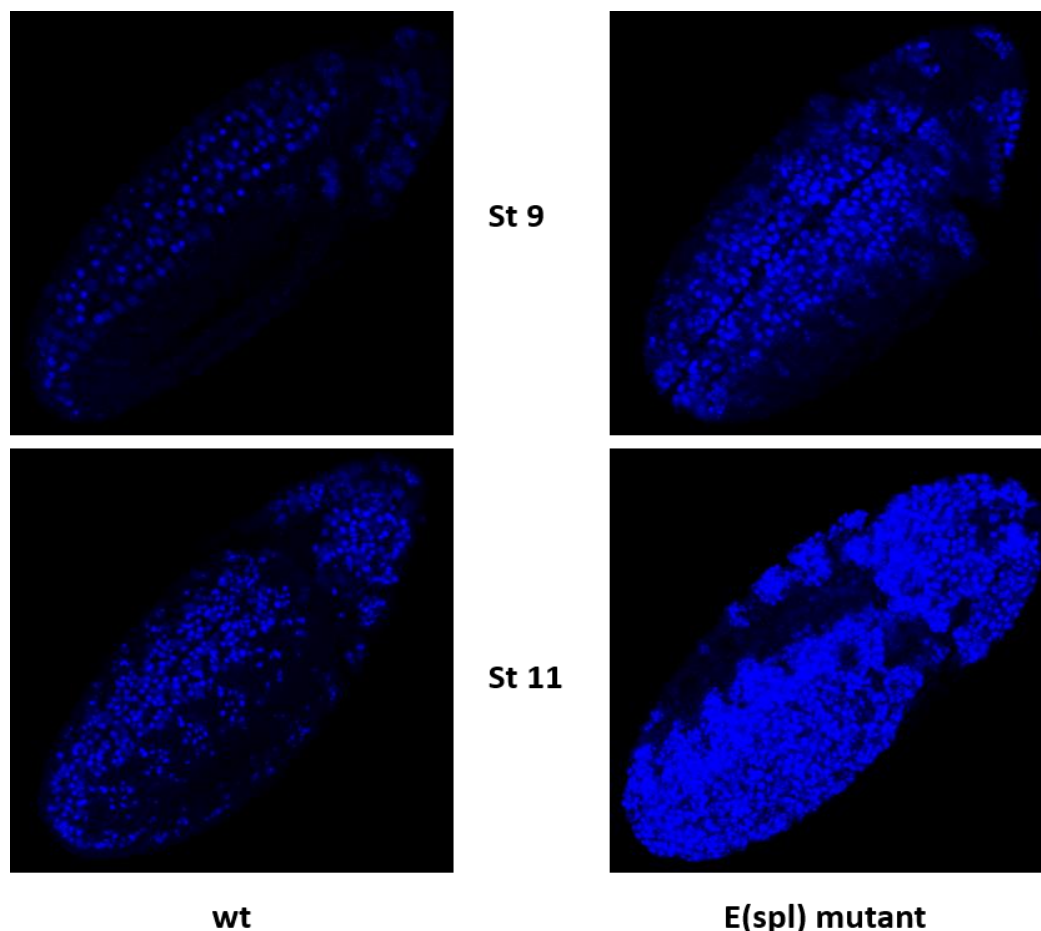


Figure 6 Excessive hypertrophies in embryonic CNS caused by the absence of E(spl) genes. Neuroblasts in wt (left) and E (spl) deficient (right) embryos. By the stage 9 deficiency of E(spl) genes promotes the generation of neural hyperplasia. Neuroblasts are being produced at the expense of epidermis. At stage 11 neuroblasts are being supernumerary and are formed ectopically.

1.6 Aim of the study

Unraveling the network of interactions that contributes to neuroblast generation at the appropriate time and space is of major importance for our understanding of the CNS development. Proneural proteins of the AS-C have been characterized as the key determinants of the neural fate selection. However, upon its deletion only a small subset of neuroblasts is lost from the CNS. How the rest of the neuroblasts manage to be formed remains poorly understood. The role of Da is equally important as indicated by the aneural phenotype observed in embryos lacking both Da and proneurals. Moreover, the finding that proneurals can act as positive regulators of E(spl) adds in the already existing complexity of their interaction and raises multiple questions. Are there other factors sustaining proneural activity or the interplay of the known ones is more perplexed than we thought? Can Da interact with other HLH factors to confer proneural activity? If so, does it have the same gene targets as in the case of its heterodimerization with proneural proteins? To address these questions, we developed two distinct approaches.

In the first approach we tried to elucidate the proneural-E(spl) interplay. Provided the hypoplastic and hyperplastic phenotypes observed in the absence of proneurals and E(spl) genes respectively, we wanted to interpret the impact of the double deletion on neuroblast formation. We also wanted to examine neuroblast divisions and *dpn* expression in double mutants. Therefore, we created flies lacking both gene complexes and studied embryos of distinct developmental stages with confocal imaging. It is shown that double mutants exhibit neural hyperplasia, milder than the one detected in the absence of E(spl) genes. Moreover, we observe a delay in *dpn* expression and a temporary arrest of neuroblasts divisions, similar to that described for the AS-C deficiency.

In the second approach we focused on the study of Da exclusively in the neuroectoderm. In the absence of both *da* and proneural, embryonic CNS completely fails to form (Figure 5A). We wanted to examine if its neuroectodermal targets coincide with those of proneurals. We tried to identify them using cHIP-sequencing and subsequently compare our results with unpublished Sc cHIP-seq data, derived from our lab. As no specific antibody recognizing Da existed, we set up a biotin pull down strategy in order to precipitate our protein along with the bound DNA. We managed to identify binding sites of Da in neuroectodermal cells which indeed overlapped with proneurals. We don't observe unique neurogenic gene targets of Da.

However, our CHIP-seq protocol needs to be further optimized in order to obtain a better understanding of Da neuroectodermal targets.

2. Materials and Methods

2.1 Fly stocks and crosses

Fly stocks used for the experiments are presented in Table 1. Stocks were used for the crosses. Sequence of fly crosses for the generation of double mutant and of the flies, bearing da, UAS-BirA are demonstrated in Figure 7.

Stocks	Source	Abbreviations	Position
FM7, Kr-Gal4 UAS-GFP/ Df(1)sc ^{B57} w sn ³		FM7, Kr-G/scB57 or scB57	1st chromosome
FM7/Df(1)sc260 w sn3		FM7/sc260	1st chromosome
w; TM3, twi- Gal4 UAS-GFP/ Dr		TM3, twi-G / Dr	3rd chromosome
w; TM3, twi- Gal4 UAS-GFP/ FRT82B e Df(3R)b32.2		TM3, twi-G/ e b32.2 or b32.2	3rd chromosome
Dp51D ; e Df(3R)b32.2			
w; da-Gal4 ^{G32}		da-Gal4	3rd chromosome
w; UAS-birA.F ²	Bloomington 58759	UAS-birA	2nd chromosome
w1118; If/CyO, wg lacz ; MKRS/TM6B, Tb1		If/CyO, MKRS/TM6B	
w; da-GFP-FPTB	Bloomington 55836		3rd chromosome
w; bib-Gal4			3rd chromosome
sox21b-Gal4			1st chromosome

Table 1 Fly stocks used for the crosses. Abbreviations of stock names are also demonstrated.

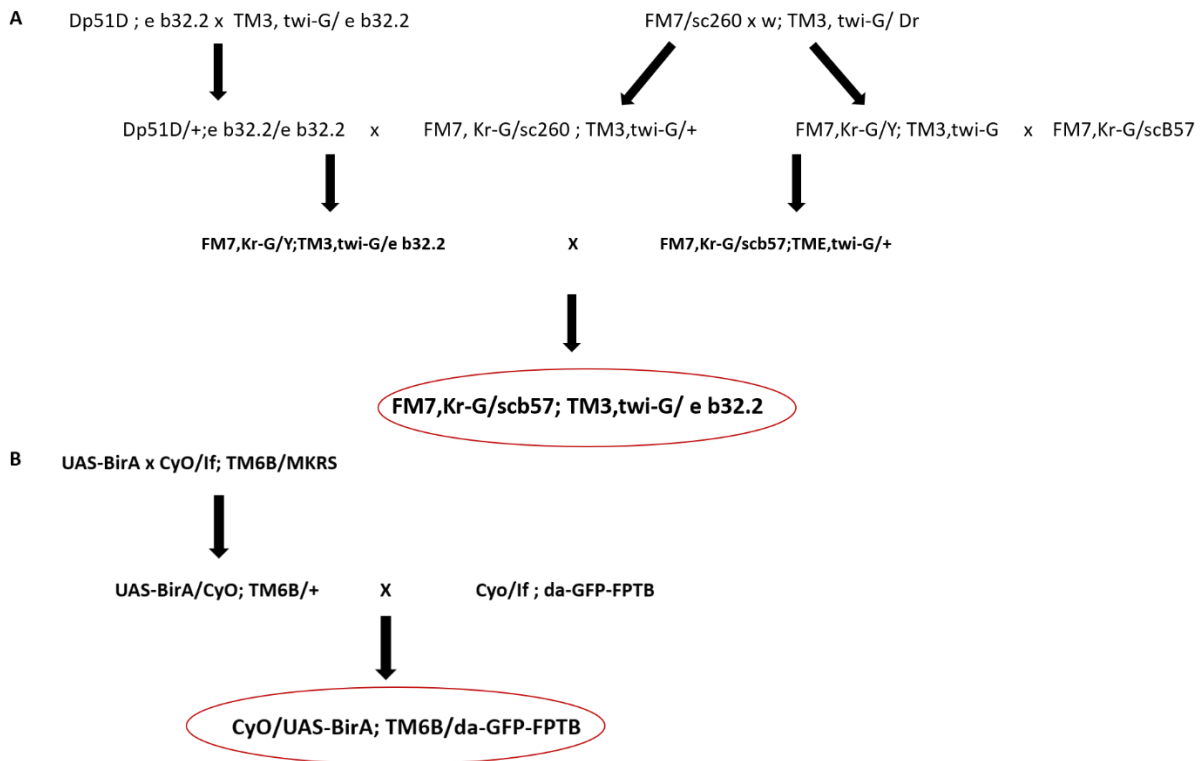


Figure 7 Sequential crosses for the generation of the stocks used in the experiments. (A) Sequential crosses to produce flies lacking both *E(spl)* and proneural genes. (B) Crosses for the generation of flies expressing the *BirA* ligase, *da* tagged with the biotin ligase recognition peptide.

2.2 Immunostaining

Embryos were dechorionated in 50% bleach for 2-5 minutes, washed with water and fixed in 4% formaldehyde/ PBS 1X for 20 minutes. Formaldehyde was discarded and removal of vitellin membrane was performed by harsh shaking in methanol solution. Crosslinked embryos were stored in methanol at -20°C. Fixed embryos were washed multiple times with PBS 1X/ 0.2% Triton X-100 (PT) and blocked for 3 hours with PBS 1X/ 1% BSA/ 0.2% Triton X-100 (PBT). Blocking buffer was removed and primary antibodies, diluted in PBT were added for O/N incubation at 4°C. Primary antibodies were discarded, embryos were washed with PT (three quick washes three 15-minute washes) and incubated with the secondary antibodies for 3-4 hours at room temperature (RT). Embryos were once again washed with PT and DAPI was added. Samples were incubated in NPG (2% n-propyl-gallate 49% glycerol and 49% PBS, pH=7.4) and mounted in 75 x 26 mm microscope slides. Slides were stored at -20°C. The following antibodies were used: rabbit anti-GFP (1/100000 MINOTECH), mouse anti-Prospero (1/100000 DSHB), Ginny pig anti-deadpan (1/100000), goat anti-rabbit Alexa Fluor® 488

(abcam, ab150077), goat anti-mouse Alexa Fluor® 555 (1/100000, Life Biotech.), goat anti-ginny pig Alexa Fluor® 647 (1/100000, Life Biotech.).

2.3 Embryo fixation for cHIP

Staged embryos (3-6 hours after egg laying (AEL)) were collected from agar plates and were incubated in 50% bleach for 3-5 minutes to remove chorion. Embryos were washed with plenty of water and were fixed in 1% formaldehyde/ PBS 1X for 10 minutes. Formaldehyde was discarded and 0,125M glycine/PBS 1X/ 0,1% Triton X-100 were added to quench any residual formaldehyde. Embryos were spined for 4 minutes at 8000 rpm, at 4°C. Supernatant was discarded, followed by two washes with ice cold PBS 1X/ 0.1% Triton X (PT). PT was removed and embryos were stored at -80°C.

2.4 Nuclear extraction

Cell lysis and nuclear isolation for chromatin immunoprecipitation (cHIP) were conducted as previously described with minor alterations ⁵¹. All treatments were performed on ice and a cocktail of protease inhibitors was added in all buffers. (cOmplete™ Protease Inhibitor Cocktail – 11697498001). Fixed embryos were resuspended in ice cold PT. After 3 washes with PBS 1X, embryos were thoroughly homogenized in a 7,5ml Wheaton dounce grinder, using a tight pestle and resulting in a single cell suspension. Solvent was transferred in 2ml Eppendorf tubes, spined at 8000rpm for 15-20 minutes at 4°C and supernatant was discarded. Pellet was resuspended in LB1 (50 mM HEPES–KOH pH 7.5, 140 mM NaCl, 1 mM EDTA, 10% Glycerol, 0.5% NP-40, 0.25% Triton X-100), incubated at 4°C for 5 minutes and centrifuged at 8000 rpm for 10 minutes at 4°C. Supernatant was removed, followed by the addition of LB2 (10 mM Tris–HCL pH8.0, 200 mM NaCl, 1 mM EDTA, 0.5 mM EGTA). Solvent was gently rocked on ice for 10 minutes and centrifuged at 8000 rpm for 10 minutes at 4°C. Supernatant was taken out and pellet was resuspended in LB3 (10 mM Tris–HCL pH 8, 100 mM NaCl, 1 mM EDTA, 0.5 mM EGTA, 0.1%Na–Deoxycholate, 0.5% N-lauroylsarcosine). Sample was split in 1,5ml Eppendorf tubes, each containing up to 300µl and sonicated in Bioruptor® Plus sonication device (Diagenode, B01020001). 8 cycles of 30 seconds ON 30 seconds OFF were performed. 1%

Triton X-100 was added in sonicated suspension and centrifugation at 13.300 rpm for 15-25 minutes at 4°C was pursued. Pelleted debris were pulled out and supernatant, containing the sheared chromatin was stored at -20°C. In each step performed, aliquots of discarded products were kept to test the efficiency of the protocol.

2.5 Chromatin pull down and sequencing

M-280 paramagnetic streptavidin beads (Invitrogen, 11205D) were used to pull down the biotinylated transcription factor along with the bound DNA. Beads were washed three times in PBS/1% BSA and resuspended in LB3 buffer. Nuclear lysates were added to the beads, mixed thoroughly and incubated O/N at 4°C. Subsequent washes of the beads with SDS Buffer (2% SDS), two times, High Salt Buffer (50 mM HEPES pH 7.5, 500 mM NaCl, 1 mM EDTA, 0.1% sodium deoxycholate, 1% Triton X-100), LiCl Buffer (10 mM Tris-HCl pH 8.1, 250 mM LiCl, 1mM EDTA, 0,5% NP-40, 0,5% sodium deoxycholate) were followed to limit non-specific binding. Alternatively, beads were washed 5-8 times with RIPA Buffer (50 mM HEPES–KOH, pH 7.5, 500 mM LiCl, 1 mM EDTA, 1% NP-40, 0.7% Na– Deoxycholate). TE (10mM Tris-HCl pH 7.5, 1mM EDTA) buffer was added and beads were centrifuged at 960g for 3 minutes at 4°C to remove residual TE. Beads as well as input sample (nuclear lysate before incubation with the beads), which stored at -20°C were incubated at 67°C for 18 hours to reverse crosslinking. Samples were centrifuged at 13300 rpm for 60 seconds. Supernatants were transferred in a new tube and left with 0,4mg/ml RNase (Thermo Scientific, EN0531) TE buffer for 30 minutes at 37°C. 0,4mg/ml Proteinase K (Invitrogen, AM2546) was added and samples were incubated at 55°C for 1-2 hours. DNA from samples was purified using the phenol-chloroform protocol. Briefly, equal volume of phenol 25: chloroform 24: isoamyl alcohol 1 (Sigma-Aldrich, P2069) was added and solutions were vortexed thoroughly. The upper phase, containing DNA was carefully isolated and 0,4M NaCl and 20µg/µl glycogen were added. DNA precipitation performed by incubation in 2 volumes 100% ethanol for 1 hour at -80°C. Samples were centrifuged at 13300rpm for 25 minutes at 4°C, supernatant was removed. 80% ethanol was added, followed by centrifugation for 15 minutes at 13300rpm at 4°C. Ethanol was discarded, pellets were left to dry and purified DNA was resuspended in 50µl elution buffer (10Mm Tris-HCl pH 8) and stored at -20°C. DNA library was constructed using the NEBNext® Ultra™ II DNA

Library Prep Kit (NEB #E7103). Samples were sequenced in Illumina Nextseq500. ChIP-seq peaks were identified using Model-based Analysis of ChIP-Seq (MACS) ⁵².

2.6 Western blot

Lysates were loaded and separated in 10% SDS-PAGE and transferred in a nitrocellulose membrane of 0.2µm pore size (BIO-RAD, 1620112). In brief, transfer sandwich was placed in the tank with 1X transfer buffer (25mM Tris, 190 mM glycine, 20% methanol, 0.1% SDS) at 100mV for 1 hour 15 minutes. Membrane was stained with Ponceau S solution (0,2% w/v Ponceau S, 5% glacial acetic acid) to check the quality of the transfer process. Ponceau was rinsed off and membrane washed three times with TBST (20 mM Tris PH 7.5, 150 mM NaCl, 0.1% Tween 20). Subsequently, it was blocked in 5% milk/ TBST for 2-3 hours. Primary antibody was diluted in 5% milk/ TBST and added to the membrane for O/N incubation at 4°C. Primary antibody was discarded and the membrane washed three times with TBST. Blot was rinsed three more times with TBST for 15 minutes and horseradish peroxidase conjugate (HRP), diluted in 5% milk/TBST was added for 2-3 hours. Secondary antibody was removed and membrane washed 3-5 times with TBST for 10 minutes. Blot was rinsed in Clarity™ Western ECL Substrate (BIO-RAD, 1705060) and the chemiluminescence signals were captured and analysed using the ChemiDoc™ Touch Imaging System (BIO-RAD). The following antibodies were used: rabbit anti-GFP (1/100000 or 1/10000, MINOTECH), Streptavidin HRP (1/1000 abcam, ab64269), rabbit anti-histone H3 (1/1000 abcam, ab1791) and Goat Anti-Rabbit IgG H&L (HRP) (1/10000 abcam, ab6721).

2.7 Quantitative PCR (qPCR)

Purified DNA fragments were analyzed by qPCR using sets of primers targeting different regions of E(spl) m4, E(spl) m8, *worniu* (*wor*), and *Ady43A* which used as control sequence. Primers sequences are the following: E(spl)-m4: F: ACGAGACTTTCTACCAGTTCC, R: CATTGTCCGTCCTCCGCTCG, E(spl)m8: F: TGAAACAATAAGCGAGTAGATGG, R: ATGCATACTTCACTGCCTCATCC, *wor*: F: TGGTTCAGCTCGTATTTCCCC, R: CGAAGAGCAAACGTCCATTAGG, 4th control: F: GGGCAAAGTCGCTCCACC, R: TGGGCATGTGTAAGCGATGC, *Ady43A* control: F: AGAGCAGGA AATCCCCAACC, R: GCCATCGCTCCAGACTGC.

3. Results

3.1 AS-C and E(spl) gene deletions lead to delayed Dpn expression and excessive neuroblast generation.

Deletion of proneural genes leads to 20-25% neuroblast loss, whereas absence of E(spl) genes results in neural hyperplasia⁴⁷. Provided the multi-scaled and complicated network of interactions between those factors, we wanted to interpret the effect of the simultaneous absence of AS-C and E(spl) genes, in neuroblast generation. We started working with fly strains lacking either AS-C genes or E(spl) genes, referred as “single mutants”. Strains were balanced with FM7 and TM3 respectively, as homozygous mutants are lethal in early stages of embryogenesis. Following a series of sequential crosses, we generated FM7, Kr-Gal4, UAS-GFP/sc^{b57}; TM3, Twi-Gal4, UAS-GFP/e b32.2 flies, which lacked both AS-C and E(spl) genes and referred as “double mutants”. GFP-expressing balancers allowed the identification of embryos lacking both gene complexes. Absence of GFP signal marked the double mutant embryos, which accounted for 1/16 of total embryos.

3.1.1 Neuroblasts are formed by the stage 8 in double mutants.

In order to obtain a holistic view of neurogenesis in double mutant embryos and to uncover the extent of interruption caused by the deletions, we examined embryos of different developmental stages, covering the whole temporal spectrum of neuroblast formation. Double mutant embryos of stage 7 -shortly after gastrulation- were studied to investigate the possibility of a premature neuroblast generation, owing to the absence of E(spl) genes. However, we didn't see untimely segregation of neural precursors, indicating that the temporal series of events have not yet been interrupted (Figure 8A). Deadpan was normally expressed in stripes and Prospero (Pros) expression was restricted in a group cephalic cells as expected (Figure 8A). Dpn expression was detected in neuroblasts, by the stage 8, in double mutants and it was limited in proneural clusters, which have been enlarged in number of cells, due to the loss of E(spl) genes and impaired lateral inhibition (Figure 8B). A hyperplastic phenotype is beginning to emerge in E(spl) single mutants, which counted more neuroblasts compared to wild type and double mutant embryos (Figure 8B). Cytoplasmic Pros was visible

in these embryos, indicating that neuroblasts are ready to divide. On the contrary, AS-C deficiency led to the decreased Dpn expression and loss of the first-wave neuroblasts (Figure 8B).

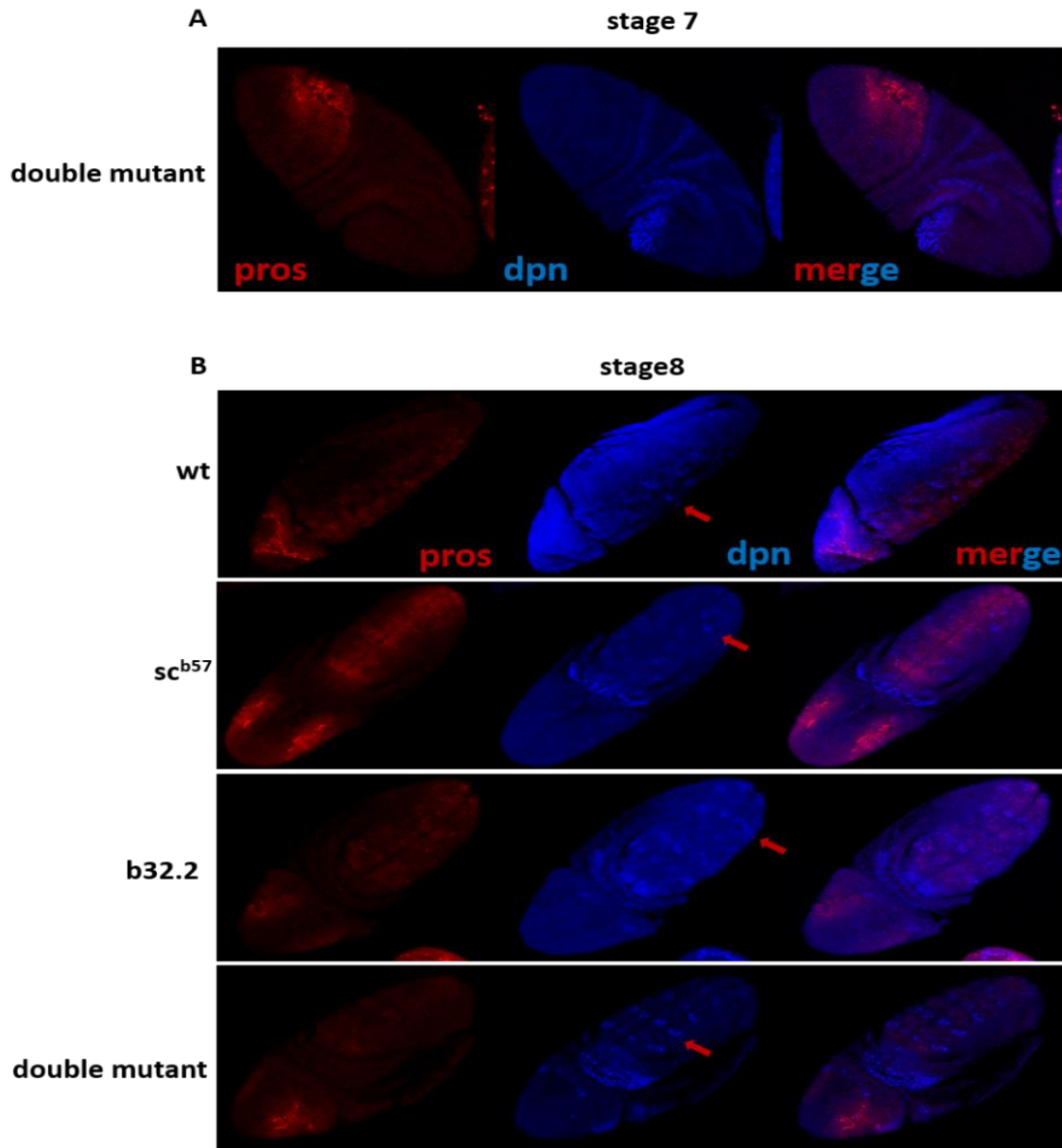


Figure 8 Impact of double deletions on embryonic stages 7 and 8. Prospero for GMCs (red), Deadpan for neuroblasts (blue) (A) Double mutant embryos of stage 7. Ablations do not lead to premature neurogenesis. Normal Dpn expression in stripes. (B) Embryos of stage 8. Arrows demonstrating neuroectodermal clusters marked with Dpn. Proneural cluster expansion to the detriment of ectodermal cells is observed both in *E(spl)* and double mutant. *AS-C* deficiency results in loss of first wave-neuroblasts as depicted by the lower Dpn levels in the clusters. A neural hyperplasia is being developed by this stage in *E(spl)* mutants. Neuroblasts have already been delaminated and the cytoplasmic localisation of Pros indicates the earlier beginning of neuroblast divisions. In double mutant embryos, neuroblasts haven't been divided.

3.1.2 Excessive generation of Dpn-negative neuroblasts in double mutants of stage 9.

Embryos of developmental stage 9 were also studied. Double mutants exhibited excessive numbers of neuroblasts, which bear cytoplasmic Pros and express little or no Dpn, denoting that the stalled neuroblast state, described for the proneural genes deficiency is also demonstrated in double mutants (Figure 9D). Provided that neuroblasts have been formed, we hypothesized that the double deletion has not disrupted the process of delamination. Only few GMCs were born at this point and we suggested that neuroblasts' divisions are paused in double mutant embryos, as it occurs in AS-C single mutants. *E(spl)* single mutants displayed severe neural hyperplasia with supernumerary neuroblasts being formed (Figure 9C). Unlike double mutants, an excess of GMCs has been generated so far (Figure 9C, 9D, 9E, 9F).

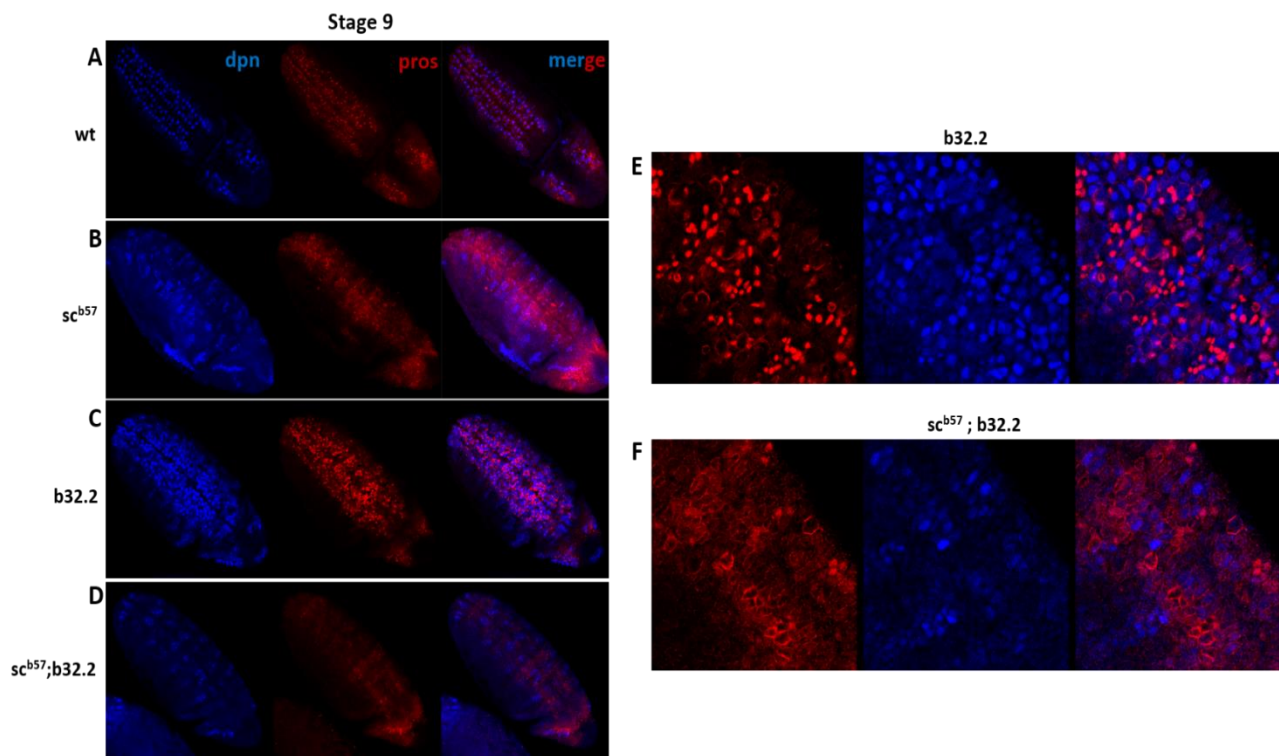


Figure 9 Lack of *dpn* expression in stage 9 double mutants. *Prospero* for GMCs (red), *Deadpan* for neuroblasts (blue). (A) wild type embryos with well-arranged arrays of neuroblasts. (B) Proneural deficiency results in decreased *Dpn* levels. Expression in neuroblasts is diminished or absent. (C) *E(spl)* deficient embryos displaying neural hypertrophy. Excessive neuroblasts and GMCs have been formed. (D) Embryo lacking both proneural and *E(spl)* genes exhibits decreased *Dpn* expression. *Dpn* phenotype closely resembles to the pattern observed in AS-C deficiency. (E) Close up of *E(spl)* single mutant at stage 9. Supernumerary neuroblasts and GMCs are demonstrated. (F) Close up of double mutant at stage 9. Spare neuroblasts are observed. Unlike the *E(spl)* mutant, the majority of neuroblasts have not been divided. Cytoplasmic *Pros* indicates that are ready to divide. Only a few GMCs are detected.

3.1.3 Embryonic stage 10 is marked by massive rebound of Dpn expression and a burst of neuroblast formation in double mutants.

A rapid burst of neuroblasts has been detected, by the stage 10, in double mutant embryos, demonstrating that cell divisions have restarted and the stalled state has been overcome (Figure 10J). Dpn expression has been restored in all neuroblasts and an excess of GMCs has been generated (Figure 10J, 10K). Unlike the previous stages, whereby double mutant neuroblast-profile resembled to proneural single mutants, at this point, severe neural hyperplasia, quite similar to that observed in E(spl) deficiencies has been revealed. Yet, the extent of hypertrophies was slighter in double mutant (Figure 10D, 10E, 10J, 10K). Embryos of developmental stage 11 sustained neuroblast production, ectopically, expanding the neurogenic phenotype in ectodermal territories (Figure 10J', 10K'). AS-C single mutant of stage 10 depicted absence of Dpn expression, which was gradually rebounded by the stage 11, as previously described (Figure 10G, 10H, 10G', 10H'). Neuroblasts rebooted its proliferation and hypoplastic phenotype was diminished.

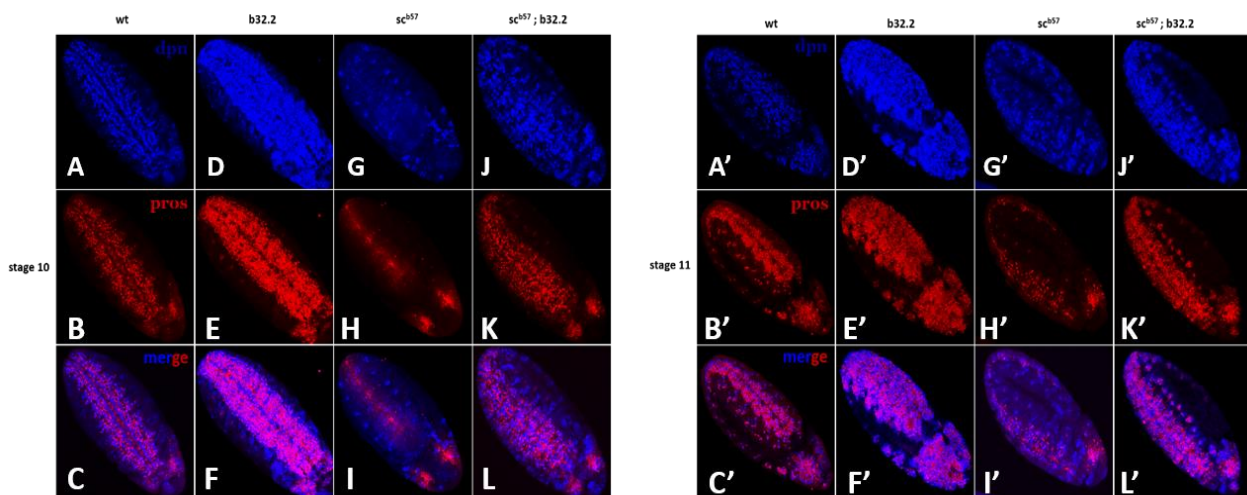


Figure 10 Neurogenic phenotype emerges in double mutant embryos in stages 10 and 11. Prospero for GMCs (red), Deadpan for neuroblasts (blue). (A-L) Stage 10 embryos, (A'-L') stage 11 embryos. (A,B,C,A',B',C') Wild type embryos of stage 10 and 11. (D,E,F,D',E',F') E(spl) deficiencies in stage 10 and 11 cause neural hypertrophies, with neuroblasts covering regions of the ectoderm and expanding laterally of the ventral nerve chord. (G,H,I) Embryos lacking AS-C genes. Dpn expression is still absent (G), GMCs haven't yet formed as Dpn-negative neuroblasts are not able to proliferate (H). (G',H',I') AS-C deficiency at stage 11. Dpn expression has been restored in neuroblasts (G'). Cell divisions have restarted and GMCs have been produced (H'). (J,K,L) Double mutant embryos of stage 10. Dpn expression is restored and a burst of neuroblast production is observed, leading to neural hyperplasia (J). Supernumerary GMCs have been formed (L). (J',K',L') Number of neuroblasts and of GMCs is increased and hypertrophies continue to grow at stage 11 double mutants.

3.1.4 Neurogenic phenotypes of double mutants at 12-13 developmental stages.

By examining double mutant embryos at later embryonic stages, we identified a gradually increasing neural hyperplasia, which continues its development (Figure 11A, 11B). Uncontrolled neuroblast proliferation was observed at *E(spl)* single mutant as well. Neuroblasts and GMCs have been produced ectopically, in superficial regions, covering the majority of embryos' ectoderm. We also observed gaps in double mutant and *E(spl)* embryos, where *Dpn* and *Pros* are not expressed. We hypothesized that these "holes" depict regions, where neurons have already been formed, replacing neuroblasts and GMCs. In proneural deficient embryos, *Dpn* expression has fully recovered and the characteristic ventral nerve chord pattern was created (Figure 11B). Even though its phenotype looks normal, it has been shown that these embryos have many functional defects in its nervous system development.

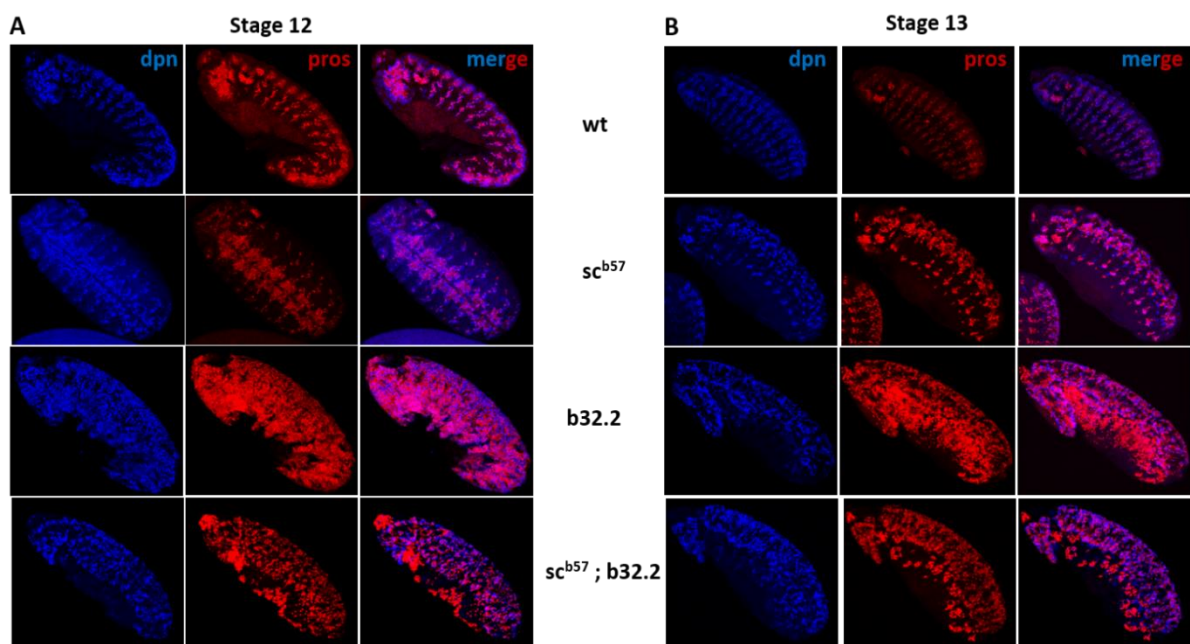


Figure 11 Neural hyperplasia continues growing in later embryonic stages. Prospero for GMCs (red), Deadpan for neuroblasts (blue). (A) wt, proneural single mutants, *E(spl)* single mutants and double mutant embryos at stage 12. Double mutants exhibit hyperplastic phenotype. *E(spl)* single mutants developed more severe hyperplasia. (B) wt, proneural single mutants, *E(spl)* single mutants and double mutant embryos at stage 13. Hypertrophies in *E(spl)* single mutants and in double mutants have covered the external regions of the embryos. Supernumerary neuroblasts and GMCs have been created.

3.2 Biotin pull-down and DNA sequencing to identify Daughterless' binding sites.

By exploiting the streptavidin-biotin strong non-polar binding as well as the UAS-Gal4 system in *Drosophila*, we attempted to set up a tissue specific pull-down assay of Da, conjugated with DNA sequencing, in order to identify its target genes exclusively in the neuroectoderm. We worked with da-GFP-FPTB fly strain, whereby Da bears a biotin ligase recognition peptide (BLRP), along with other tagged epitopes. BLRP is recognized by BirA ligase, resulting in the addition of biotin molecules in the transcription factor. A Gal4 line was used to drive the overexpression of BirA gene in neuroectodermal regions. In response to BirA expression, Da was biotinylated specifically in cells of the neuroectoderm.

3.2.1 Selection of Gal4 driver to promote the expression in the neuroectoderm

We screened three different Gal4 lines using UAS-CD8-GFP as reporter gene, in order to determine which one fulfils the following requirements: a) expression in early stages, similar to the neuroblast generation time window, b) sharp expression in the neuroectoderm and c) maintenance of strong signal. It was shown that the bib-Gal4 driver utterly met those criteria and thus it was selected for the following experiments. Unlike the restricted expression of sox21b-Gal4 in the medial neuroectoderm and the ubiquitous pattern of da-Gal4, bib-Gal4 also covers the lateral neuroectodermal territory, though being limited in this region (Figure 12B and 12C).

3.2.2 Daughterless pull-down assays.

UAS-birA/UAS-birA; da-GFP.FPTB/ da-GFP.FPTB strain was crossed to bib-Gal 4 flies (Figure 12A). Embryos of 3-6 hours after egg laying (AEL), responding to 8-11 developmental stages, were collected and nuclear protein extracts were prepared. Initially we evaluated the approximate molecular weight of our protein by western blotting against GFP (Figure 12D). Subsequently we proceeded to pull down assays, using streptavidin paramagnetic beads. It was shown that biotinylated Da was efficiently precipitated in the beads. Yet, protein was also detected in whole cell extracts, indicating either cytoplasmic localization of the biotinylated protein or nuclear losses during the extraction protocol (Figure 12E). Western blots were conducted, using streptavidin-horseradish peroxidase (HRP) conjugates to validate the

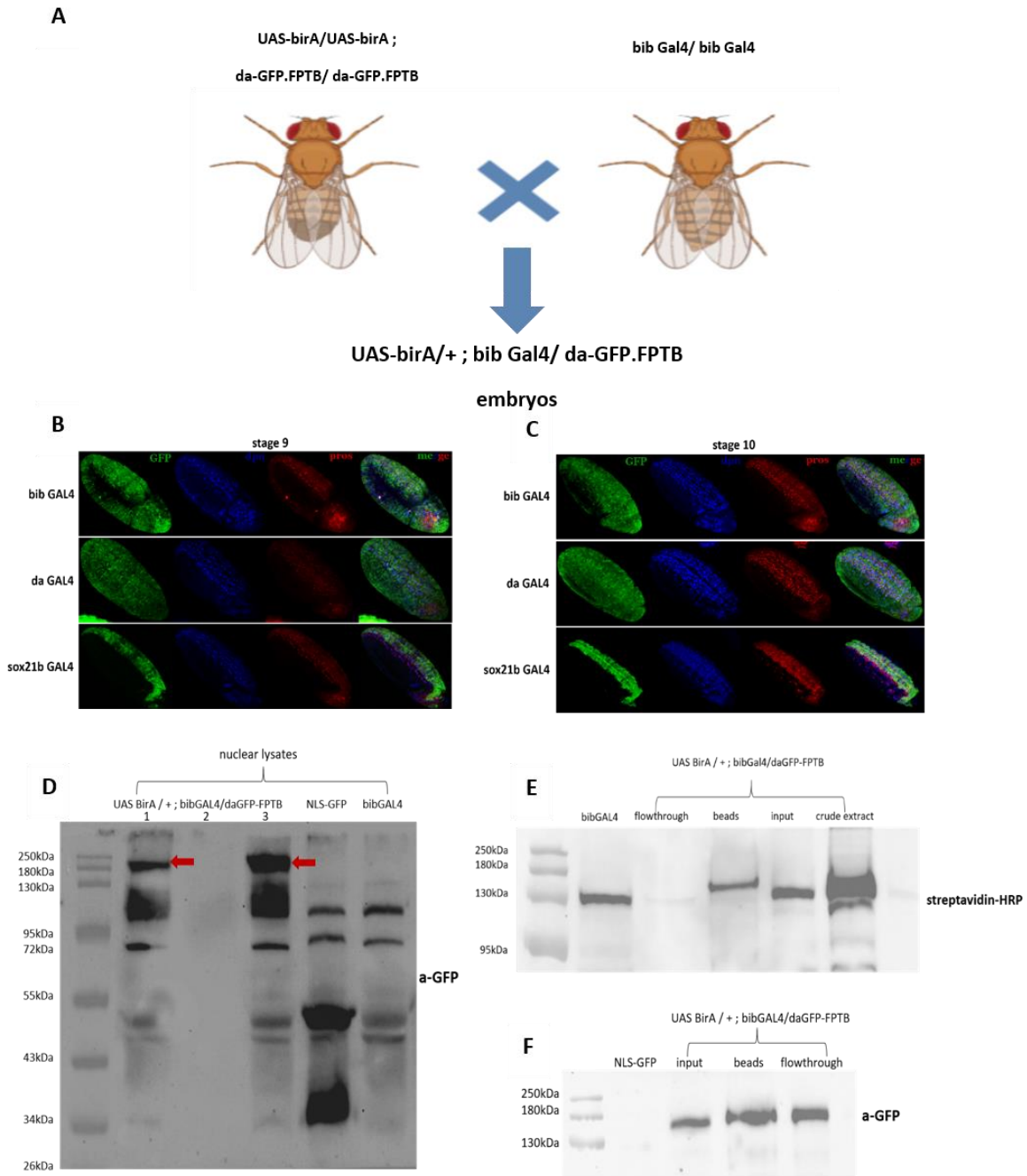


Figure 12 Biotin pull-down assay: Crossing of *UAS-birA/UAS-birA ; da-GFP.FPTB/ da-GFP.FPTB* to *bib-Gal4* flies led to the production of *UAS-birA/+ ; bib Gal4/ da-GFP.FPTB*, in which BirA ligase is specifically expressed in neuroectoderm and adds biotin peptides in tagged *Da* protein. (A) Cross set up to produce embryos carrying *UAS-birA*, *bib-Gal4* and *da-GFP-FPTB* (B) *UAS-CD8-GFP* as a reporter gene for *Gal4* driver selection. *bib-Gal4* drives restricted GFP expression in neuroectoderm. GFP (green) signal is visible by the stage. (C) GFP signal remains strong in later stages. Dpn (blue) marks neuroblasts and Pros (red) for GMCs (D) Biotinylated Daughterless-GFP-FPTB is detected at 140-180kDa. NLS-GFP fly strain was used as positive control and *bib-Gal4* strain as a negative control for *a-GFP* activity. (E) Western blot with streptavidin-HRP conjugate. Biotinylated Daughterless-GFP-FPTB is effectively pulled down by streptavidin beads. Protein is also detected in crude extracts from whole cell lysates. Non-specific binding of streptavidin in endogenously biotinylated enzymes is observed. (F) Western blot against GFP. Detection of biotinylated Daughterless-GFP-FPTB in beads. Detection in flowthrough depicts *Da* in tissues other than neuroectoderm as it is ubiquitously expressed.

efficiency of the biotinylation process. As biotinylated enzymes are endogenously produced in *Drosophila*, non-specific interactions were expected to be observed in molecular weights similar to that of biotinylated Da (Figure 12E). To avoid obtaining a false positive signal, caused by non-specific binding of those enzymes, western blot against GFP was performed, thereby enabling the cross-validation of the pull-down efficiency and specificity in an unbiased context (Figure 12F). Indeed, our results coincided, demonstrating that our protocol successfully led to the precipitation of the Da-GFP-FPTB and eliminated non-specific interactions.

3.2.3 Identification of Daughterless neuroectodermal gene targets.

Since the efficiency of biotin pull-down has been evaluated, we proceeded to the purification of bound DNA, followed by qPCR. Sequences of well-characterized Da targets were selected,

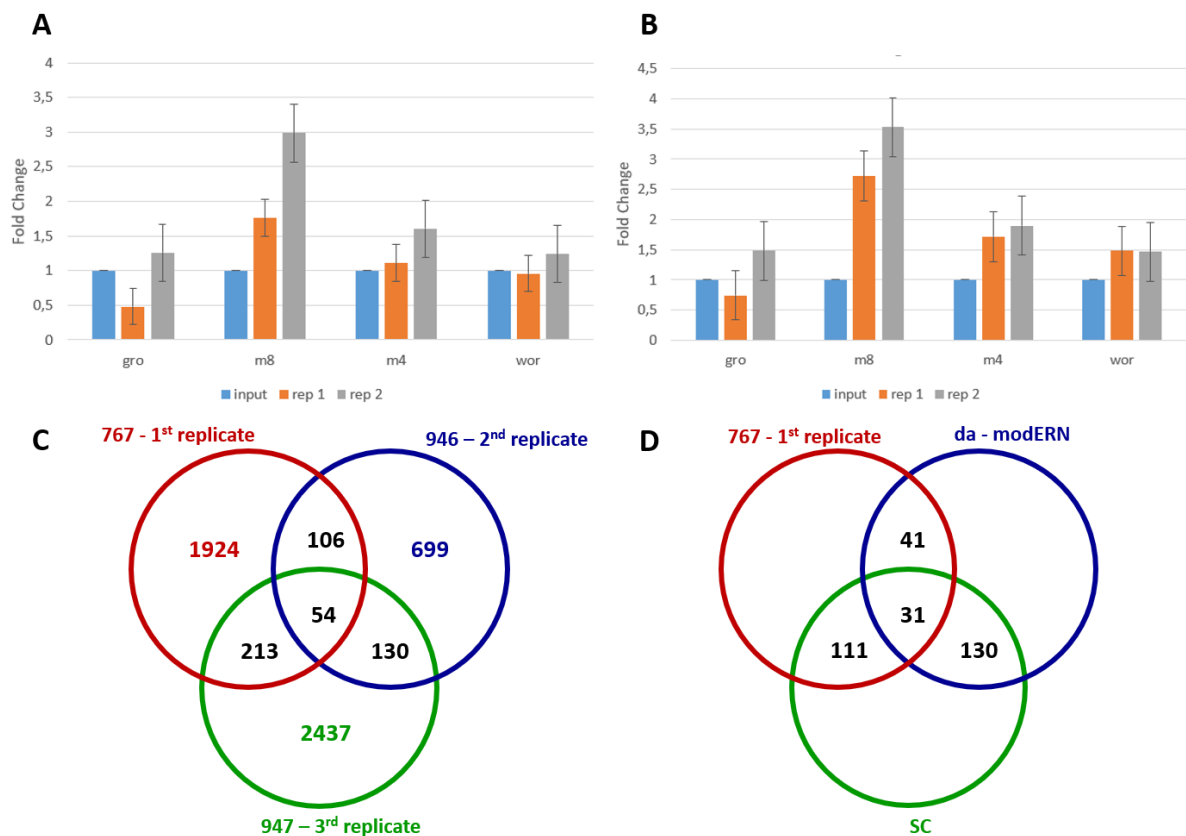


Figure 13 q-PCR and Da CHIP-seq: (A), (B) q-PCR using sets of primers, targeting different regions of groucho, E(spl) m8 and m4 and wormiu. Input DNA (blue), first replicate (orange), second replicate (grey). (A) Normalization over control sequence of Ady 43A, (B) of the 4th chromosome. Sequences are enriched with m8, demonstrating the highest enrichment. (C), (D) Intersection of CHIP-seq peaks. (C) Overlapping regions with high peaks among three replicates that were sequenced. 54 common sites identified. (D) Overlapping peaks among first replicate, Sc-CHIP-seq (unpublished work) and Da-CHIP-seq from whole embryos (published study). In total, 31 common sites were found.

enabling us to test our samples. Enrichment was observed in all known Da binding sites, as expected (Figure 13A and 13B). Particularly, m8 and m4 sequences were highly enriched in our samples compared to the input sample. Groucho and wormiu sequences displayed a milder enrichment.

Having already strong indications that our protocol efficiently led to the precipitation of biotinylated Da along with its bound DNA, we proceeded with DNA sequencing in order to identify the target sites of our protein. Three replicates were prepared and sent for sequencing. All of our replicates resulted in low enrichment binding peaks with a strong background, making the dissection of useful information about the target genes difficult. We found that 54 sites overlapped in all three replicates (Figure 13C). Sites were mapped and the neighboring genes were identified and presented at Table 2.

Given the small number of the intersected sequences, we decided to validate our results by mining and comparing data from a published cHIP-seq experiment of Da, deriving from whole embryos. We also took advantage of an unpublished cHIP-seq study, conducted in our laboratory, against Daughterless' interactor, Scute. We chose to compare these data with our first replicate, as we have noticed that it yields the lowest background among the three replicates. We discovered 41 common sites between our sample and the whole embryo Da-cHIP-seq and 111 sequences with Sc-cHIP-seq (Figure 13D). Out of the 41 overlapping sites, 31 were found to be common in all experiments, indicating that our results are valid (Figure 13D). Table 3 demonstrates the concomitant genes for the identified sequences.

Among the enriched sequences found to overlap, we identified that regions of cis regulatory elements related to E(spl) m4 and E(spl) m8 were included in our list (Figure 14A). These sites exhibited the largest enrichment peaks in our experiments and represent well-known Da

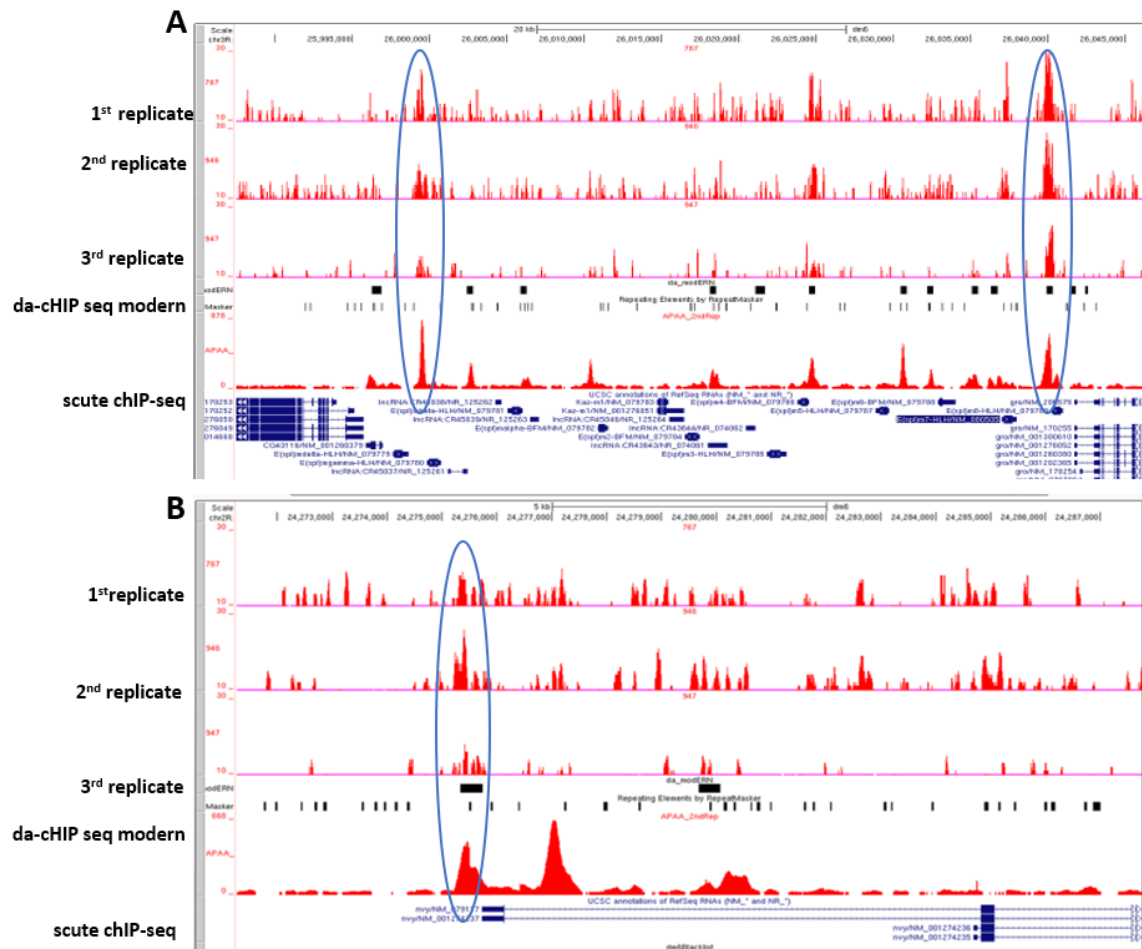


Figure 14 Predicted binding sites of *Da* in *E(spl) m8*, *E(spl) m4* and *nery (nvy)* regulatory elements. Screenshots from the UCSC Genome Browser including data from sequencing of our replicates and whole embryo *Da* chIP-seq and Scute chIP-seq. (A) Peaks in regulatory sites of *E(spl)* locus. Sequences of *m8* and *m4* were enriched in our samples, coinciding with published *Da* chIP-seq and Scute chIP-seq conducted in our laboratory. (B) Enhancer of *nery (nvy)* is also predicted as *Da* binding site.

targets, denoting that the signal obtained was real rather than the outcome of the strong background. We identified a regulatory sequence of *nery (nvy)* gene, which also depicts a known target of *Da* that is highly enriched in our replicates. (Figure 14B).

By closer examination in our overlapping sequences, regulatory sequences of *inscuteable (insc)* and *brat* genes were detected as putative *Da* binding sites (Figure 15A, 15B). Products derived from those genes are implicated in the asymmetric cell divisions of neuroblasts.

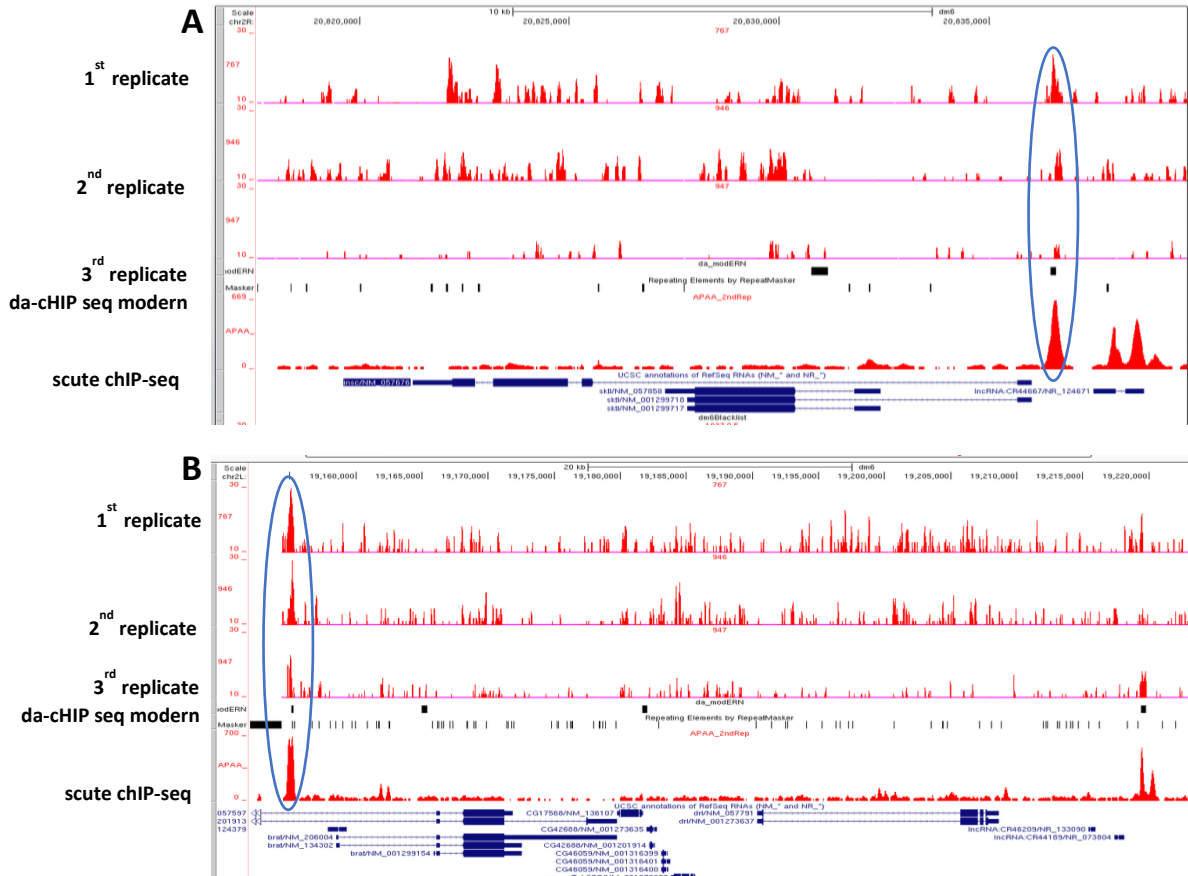


Figure 15 Predicted binding sites of *Da* in enhancers of *insc* and *brat*. Screenshots from the UCSC Genome Browser including data from sequencing of our replicates and whole embryo *Da* cHIP-seq and *Scute* cHIP-seq. (A) *Insc* and (B) *Brat* enhancers found to be enriched. Our third replicate is showing slighter enrichment compared to the others, possibly owing to technical handling.

Inscuteable is distributed in daughter cells that retain the stem cell fate, whereas *Brat*, along with *Pros* are localized in the newly born GMC, leading to the inhibition of self-renewal and promotion of the cell differentiation into neurons⁵³. Our data are in line with previous studies suggesting that our pulldown technique is effective and provides specificity.

Gene Name	Annotation	Distance to TSS	Nearest PromoterID
CG43149	Intergenic	6635	NM_001259591
scrt	Intergenic	-3953	NM_079187
Pzl	intron (NM_001316564, intron 11 of 20)	230063	NM_001316564
sxc	Intergenic	-5538	NM_078896
asRNA:CR31429	intron (NM_001170092, intron 1 of 2)	2846	NR_048350
Maf1	exon (NM_001300720, exon 3 of 4)	725	NM_001300720
JMJD4	intron (NM_001299103, intron 15 of 15)	-2719	NM_001299102
msi	intron (NM_001260374, intron 5 of 6)	1984	NM_079838
Sgs1	exon (NM_078751, exon 2 of 2)	1014	NM_078751
CG17362	exon (NM_176328, exon 6 of 6)	-3847	NM_140419

mir-9381	TTS (NM_001104425)	-8763	NR_144664
Svil	exon (NM_206242, exon 4 of 10)	3614	NM_001299985
sxc	Intergenic	-5538	NM_078896
JMJD4	3' UTR (NM_165245, exon 15 of 15)	-1765	NM_001299102
CG7724	exon (NM_001104161, exon 10 of 10)	21182	NM_140700
CG3107	Intergenic	14478	NM_001043005
Set1	Intergenic	-33815	NM_001170377
Maf1	intron (NM_001015167, intron 1 of 5)	-1419	NM_001015168
lncRNA:CR43437	Intergenic	-6504	NR_047708
JMJD4	intron (NM_001299103, intron 15 of 15)	-2719	NM_001299102
Sfp33A1	Intergenic	-14222	NM_001169484
Muc14A	exon (NM_167482, exon 4 of 14)	9235	NM_167482
Oaz	intron (NM_001202000, intron 1 of 5)	2530	NM_001202000
JMJD4	intron (NM_001299103, intron 15 of 15)	-2719	NM_001299102
CG42784	exon (NM_001201869, exon 4 of 9)	14181	NM_001259092
mir-2493	promoter-TSS (NR_048392)	-333	NR_048392
Thd1	exon (NM_143668, exon 6 of 6)	11834	NM_001297786
lncRNA:CR43951	promoter-TSS (NR_073940)	64	NR_073940
lncRNA:CR44189	Intergenic	2042	NR_073804
trbl	Intergenic	-1182	NM_079933
RYa	Intergenic	-47214	NM_001110912
CG18081	TTS (NM_140550)	1311	NM_001259848
Atf6	exon (NM_001316406, exon 20 of 20)	31110	NM_136315
E(spl)m8-HLH	promoter-TSS (NM_079789)	-239	NM_079789
d4	Intergenic	5984	NM_136319
lncRNA:flam	TTS (NR_133538)	7130	NR_133536
RYa	Intergenic	-124782	NM_001110912
Maf1	3' UTR (NM_001110544, exon 6 of 6)	3894	NM_001300720
Sgs1	exon (NM_078751, exon 2 of 2)	1717	NM_078751
lncRNA:CR44217	Intergenic	-3256	NR_073820
Muc12Ea	exon (NM_167403, exon 1 of 4)	1439	NM_167403
pk	exon (NM_165512, exon 3 of 7)	22236	NM_165512
RYa	Intergenic	-124782	NM_001110912
nvd	intron (NM_001104200, intron 2 of 5)	26518	NM_001104200
asRNA:CR44370	non-coding (NR_124559, exon 3 of 6)	773	NR_124558
JMJD4	3' UTR (NM_165245, exon 15 of 15)	-1765	NM_001299102
Cdk1	promoter-TSS (NM_078813)	254	NM_057449
gus	Intergenic	13665	NM_165422
CG14044	exon (NM_078751, exon 2 of 2)	-1943	NM_135035
Tim23	Intergenic	-60817	NM_001015387
d4	Intergenic	5077	NM_136319
gus	Intergenic	12841	NM_165422
nvd	exon (NM_001104200, exon 2 of 6)	23520	NM_001104200
Maf1	5' UTR (NM_001110544, exon 2 of 6)	247	NM_001015168

Table 2: Genes neighboring the identified sequences. 54 enriched sites were found to overlap in our replicates. Genes related to these sites are presented in the first column. Annotation of each enriched sequence, positional information and the ID of the closest promoter to these sites are depicted in second, third and fourth column respectively.

Gene Name	Annotation	Distance to TSS	Nearest PromoterID
Acf	promoter-TSS (NM_170577)	783	NM_080486
nmo	intron (NM_001370048, intron 2 of 7)	5870	NM_168248
Kdm4B	intron (NM_176164, intron 1 of 5)	3153	NM_001169668

insb	promoter-TSS (NM_137372)	83	NM_001299602
Kdm4B	intron (NM_176164, intron 1 of 5)	1155	NM_001169666
brat	intron (NM_001201913, intron 2 of 4)	-3504	NM_206004
CG6005	exon (NM_169845, exon 5 of 6)	6186	NM_142514
Sik3	promoter-TSS (NM_137517)	177	NM_001202040
lncRNA:CR43951	promoter-TSS (NR_073940)	79	NR_073940
Ran	promoter-TSS (NM_143712)	-91	NM_143712
E(spl)m8-HLH	promoter-TSS (NM_079789)	-233	NM_079789
alphaTub84B	TTS (NM_057424)	2985	NM_057424
lncRNA:CR44189	Intergenic	2011	NR_073804
lncRNA:CR45677	intron (NM_079933, intron 1 of 1)	-2593	NR_125016
asRNA:CR31429	intron (NM_001170092, intron 1 of 2)	2857	NR_048350
Wwox	intron (NM_001298806, intron 3 of 6)	2274	NM_001298806
CG3788	promoter-TSS (NM_137894)	-306	NM_001202062
msi	intron (NM_001260374, intron 5 of 6)	2123	NM_079838
Tailor	promoter-TSS (NM_169169)	118	NM_001275398
LanB1	intron (NM_057270, intron 1 of 4)	358	NM_057270
cact	promoter-TSS (NM_205999)	60	NM_057595
trx	intron (NM_057422, intron 1 of 7)	3072	NM_001014621
trbl	Intergenic	-1263	NM_079933
insc	promoter-TSS (NR_124671)	-500	NM_057676
cic	promoter-TSS (NM_080253)	-341	NM_001260275
CalpA	promoter-TSS (NM_166351)	303	NM_057699
Alh	intron (NM_001275400, intron 5 of 9)	2316	NM_169172
Ndfip	promoter-TSS (NM_140743)	193	NM_168743
ban	non-coding (NR_048209, exon 1 of 1)	1473	NR_048212
Shrm	intron (NM_166047, intron 1 of 3)	1236	NM_166047
nvy	promoter-TSS (NM_079117)	-145	NM_001274237

Table 3 Common Daughterless gene targets identified by the intersection of our first replicate to whole-embryo Da cHIP-seq and to Scute cHIP-seq. First column demonstrates the names of genes found to be related to the enriched sites. Annotation of each enriched sequence, positional information and the ID of the closest promoter to these sites are depicted in second, third and fourth column respectively.

4. Discussion

During the current study we tried to obtain a better knowledge of the molecular events contributing to the embryonic neurogenesis. In order to gain these insights, we developed a binary approach, incorporating imaging, genetic and biochemical tools. We generated embryos lacking both proneural and E(spl) genes. We also performed cHIP-seq against Da to identify its gene targets specifically in the neuroectoderm.

4.1 Proneurals and E(spl) promote its defects independently

We have asked if proneural-E(spl) interaction is more perplexed than we thought. Given the multi-level repression conferred by E(spl) and the autoregulatory mechanisms generated by proneurals to maintain its activity, we wanted to examine what would be the effect on neuroblast formation if both of them were absent. We report a hyperplastic phenotype in double mutant embryos, being different to that observed in E(spl) mutations though. Loss of proneurals cannot reverse or balance this neurogenic phenotype. It can be suggested that double deletion results in an intermediate effect in neuroblasts formation. Generation of supernumerary neuroblasts depicts E(spl) defects, while loss of *dpn* expression constitutes a trait owing to the absence of proneurals. Therefore, it is proposed that loss of these complexes promote its defective phenotypes independently. Although, additional studies should be conducted in order to understand how these complexes are connected and untangle its relationship. In our experiments we mainly focused on the qualitative effects, caused by the loss of AS-C and E(spl) complex. The development of a quantitative method, that will allow us to count neuroblasts as well as the *dpn* expression within them will provide significant insights to our study.

4.2 The role of *dpn* in embryonic neuroblasts

During development, the correct timing of biological processes is one of the major prerequisites in order for an organism to be properly settled. The *dpn* expression delay observed in double mutants and the temporary arrest of divisions, may depict the cause of the devastating defects arising on later stages of embryonic neurogenesis. Although *dpn* role is well recapitulated in the development of the larval CNS, little is known about its putative

functions during embryogenesis. Unpublished Sc cHIP-seq data from our lab shows that *dpn* constitutes a proneural target. However, it is well known that proneurals are not the only activators of *dpn*⁵⁴. In other contexts, *dpn* expression can also be induced by Notch signalling⁵⁵. Proneural-independent expression of *dpn* also seems to be the case in embryonic neuroblasts, as indicated in our experiments, whereby *dpn* is activated even upon proneural absence. A hypothesis that could be made is that proneurals activate *dpn* exclusively during the first waves of neuroblast generation. At later stages *dpn* is induced in neuroblasts through other mechanisms. However, this minor disruption in the timing of *dpn* expression, due to loss of proneural genes, is sufficient to trigger such a great impairment in the nervous system development. Though, more research should be done in order to verify this theory. Elucidation of *dpn* insights is of great importance for understanding the mechanisms that govern neuroblast commitment and proliferation.

4.3 Understanding the role of *Da* in embryonic neurogenesis

We also studied the role of *Da* in the neuroectoderm. In an effort to understand if *Da* can act separately from proneural genes to activate neural fate, we performed a cHIP-seq to identify its gene targets in neuroectoderm. We wanted to examine the possibility of inducing distinct gene targets. Even though we managed to cross-validate our results and verify the efficiency of our pull-down assay, we were not able to find unique *Da* targets. To understand if this is the real case, we need to proceed in additional experiments. The identification of *Da* interactors specifically in the neuroectoderm will constitute a complementary approach, that will help us elucidate if *Da* heterodimerizes with other factors, retaining proneural activity. Thus, the development of a proteomic based approach is needed to allow us the identification of additional *Da* interactors. Provided that *Da* is expressed uniformly in the embryos, we need to incorporate to these experiments the tissue specificity. Our biotin-based strategy as well as the UAS-Gal4 system can also be used in this context in order to identify *Da* interactors specifically in the neuroectoderm.

4.4 Technical improvement of our protocol will provide robustness in our pull-down method

It is also of utter need to improve our protocol, in order to obtain results of higher quality and lower background. The first thing that can be optimized is the nuclear extraction protocol. We observed a loss of sample during homogenization of the embryos that can be improved by milder treatments, using for example a gentler approach to homogenize. A second cause of the low enrichment yield may be due to a reduced DNA material used for sequencing. To overcome this obstacle, we have to start with greater number of embryos. A third hypothesis we made is that a big quantity of biotinylated Da is remaining in the cytoplasm and does not enter the nucleus. Therefore, our nuclear prep contains biotinylated Da in low concentrations. Given the low turnover of Da and thus its great stability, there is possibility that maternal derived Da is emerging during the first stages of early neurogenesis. In order to solve this problem, we have to reset our crossing strategy. In our experiments we crossed males containing Da, fused with the BLRP tag. However, if we select females from this stock, embryos of the next generation will carry the maternal Da with the tag and thus it will be biotinylated. We believe that optimization of these steps will allow us to obtain a better resolution and by repeating the experiment to gain a better understanding of Da binding sites. Nevertheless, improvement of our protocol is of great importance, as it can be widely used for the study of other transcription factors bearing the BLRP.

5. Bibliography

1. Nüsslein-volhard, C. & Wieschaus, E. Mutations affecting segment number and polarity in drosophila. *Nature* **287**, 795–801 (1980).
2. Harding, K. & White, K. Drosophila as a model for developmental biology: Stem cell-fate decisions in the developing nervous system. *J. Dev. Biol.* **6**, (2018).
3. Fernández-Hernández, I., Rhiner, C. & Moreno, E. Adult Neurogenesis in Drosophila. *Cell Rep.* **3**, 1857–1865 (2013).
4. Li, G. & Hidalgo, A. Adult neurogenesis in the drosophila brain: The evidence and the void. *Int. J. Mol. Sci.* **21**, 1–14 (2020).
5. Prokop, A. & Technau, G. M. The origin of postembryonic neuroblasts in the ventral nerve cord of Drosophila melanogaster. *Development* **111**, 79–88 (1991).
6. Green, P., Hartenstein, A. Y. & Hartenstein, V. The embryonic development of the Drosophila visual system. *Cell Tissue Res.* **273**, 583–598 (1993).
7. Homem, C. C. F. & Knoblich, J. A. Drosophila neuroblasts: A model for stem cell biology. *Dev.* **139**, 4297–4310 (2012).
8. Holguera, I. & Desplan, C. Neuronal specification in space and time. *Science (80-.).* **362**, 176–180 (2018).
9. Muller, H. J. & Prokofyeva, A. A. The Individual Gene in Relation to the Chromomere and the Chromosome. *Proc. Natl. Acad. Sci.* **21**, 16–26 (1935).
10. Raffel, D. & Muller, H. J. POSITION EFFECT AND GENE DIVISIBILITY CONSIDERED IN CONNECTION WITH THREE STRIKINGLY SIMILAR SCUTE MUTATIONS. *Genetics* (1940).
11. GARCfA-BELLIDO, A. Genetic Analysis of the Achaete-Scute System. *Genetics* **91**, 491–520 (1979).
12. WHEELER, W. M. NEUROBLASTS I N THE ARTHROPOD EMBRYO. (CLARK UNIVERSITY, WORCES, 1891). doi:10.4324/9781315621685-58.
13. Doe, C. Q. Molecular markers for identified neuroblasts and ganglion mother cells in the Drosophila central nervous system. *Development* **116**, 855–863 (1992).
14. Skeath, J. B. & Thor, S. Genetic control of Drosophila nerve cord development. *Curr. Opin. Neurobiol.* **13**, 8–15 (2003).
15. Lawrence, P. A., Sanson, B. & Vincent, J. P. Compartments, wingless and engrailed: Patterning the ventral epidermis of Drosophila embryos. *Development* **122**, 4095–4103 (1996).
16. Weiss, J. B. *et al.* Dorsoventral patterning in the Drosophila central nervous system: the intermediate neuroblasts defective homeobox gene specifies intermediate column identity. *GENES Dev.* **12**, 3591–3602 (1998).
17. McDonald, J. A. *et al.* Dorsoventral patterning in the Drosophila central nervous system: The vnd homeobox gene specifies ventral column identity. *Genes Dev.* **12**, 3603–3612 (1998).
18. Isshiki, T., Takeichi, M. & Nose, A. The role of the msh homeobox gene during Drosophila neurogenesis: Implication for the dorsoventral specification of the neuroectoderm. *Development* **124**, 3099–3109 (1997).

19. Isshiki, T., Pearson, B., Holbrook, S. & Doe, C. Q. Drosophila neuroblasts sequentially express transcription factors which specify the temporal identity of their neuronal progeny. *Cell* **106**, 511–521 (2001).
20. Grosskortenhaus, R., Pearson, B. J., Marusich, A. & Doe, C. Q. Regulation of temporal identity transitions in drosophila neuroblasts. *Dev. Cell* **8**, 193–202 (2005).
21. Jiménez, F. & Campos-Ortega, J. A. A region of the Drosophila genome necessary for CNS development [23]. *Nature* **282**, 310–312 (1979).
22. Knust, E., Tietze, K. & Campos-Ortega, J. A. Molecular analysis of the neurogenic locus Enhancer of split of Drosophila melanogaster. *EMBO J.* **6**, 4113–4123 (1987).
23. Artavanis-Tsakonas, S., Rand, M. D. & Lake, R. J. Notch signaling: Cell fate control and signal integration in development. *Science (80-.)*. **284**, 770–776 (1999).
24. Heitzler, P., Bourouis, M., Ruel, L., Carteret, C. & Simpson, P. Genes of the Enhancer of split and achaete-scute complexes are required for a regulatory loop between Notch and Delta during lateral signalling in Drosophila. *Development* **122**, 161–171 (1996).
25. Fortini, M. E. & Artavanis-Tsakonas, S. The suppressor of hairless protein participates in notch receptor signaling. *Cell* **79**, 273–282 (1994).
26. Kitagawa, M. Notch signalling in the nucleus: Roles of Mastermind-like (MAML) transcriptional coactivators. *J. Biochem.* **159**, 287–294 (2015).
27. Villares, R. & Cabrera, C. V. The achaete-scute gene complex of D. melanogaster: Conserved Domains in a subset of genes required for neurogenesis and their homology to myc. *Cell* **50**, 415–424 (1987).
28. Gonzalez, F., Romani, S., Cubas, P., Modolell, J. & Campuzano, S. Molecular analysis of the asense gene, a member of the achaete-scute complex of Drosophila melanogaster, and its novel role in optic lobe development. *EMBO J.* **8**, 3553–3562 (1989).
29. Jarman, A. P., Grau, Y., Jan, L. Y. & Jan, Y. N. atonal is a proneural gene that directs chordotonal organ formation in the Drosophila peripheral nervous system. *Cell* **73**, 1307–1321 (1993).
30. Goulding, S. E., Lage, P. zur & Jarman, A. P. amos, a proneural gene for Drosophila olfactory sense organs that is regulated by lozenge. *Neuron* **25**, 69–78 (2000).
31. Goulding, S. E., White, N. M. & Jarman, A. P. cato encodes a basic helix-loop-helix transcription factor implicated in the correct differentiation of Drosophila sense organs. *Dev. Biol.* **221**, 120–131 (2000).
32. Johnson, J. E., Birren, S. J. & Anderson, D. J. Two rat homologues of Drosophila achaete-scute specifically expressed in neuronal precursors. *Nature* **346**, 858–861 (1990).
33. Skeath, J. B., Panganiban, G. F. & Carroll, S. B. The ventral nervous system defective gene controls proneural gene expression at two distinct steps during neuroblast formation in Drosophila. *Development* **120**, 1517–1524 (1994).
34. Murre, C. *et al.* Interactions between heterologous helix-loop-helix proteins generate complexes that bind specifically to a common DNA sequence. *Cell* **58**, 537–544 (1989).
35. Cline, T. W. A sex specific, temperature sensitive maternal effect of the daughterless mutation of Drosophila melanogaster. *Genetics* **84**, 723–742 (1976).

36. Caudy, M. *et al.* daughterless, a Drosophila gene essential for both neurogenesis and sex determination, has sequence similarities to myc and the achaete-scute complex. *Cell* **55**, 1061–1067 (1988).
37. Vaessin, H., Brand, M., Jan, L. Y. & Jan, Y. N. daughterless is essential for neuronal precursor differentiation but not for initiation of neuronal precursor formation in Drosophila embryo. *Development* **120**, 935–945 (1994).
38. Dennis, D. J., Han, S. & Schuurmans, C. bHLH transcription factors in neural development, disease, and reprogramming. *Brain Res.* **1705**, 48–65 (2019).
39. Ellis, H. M., Spann, D. R. & Posakony, J. W. extramacrochaetae, a negative regulator of sensory organ development in Drosophila, defines a new class of helix-loop-helix proteins. *Cell* **61**, 27–38 (1990).
40. Wurmbach, E., Wech, I. & Preiss, A. The enhancer of split complex of Drosophila melanogaster harbors three classes of Notch responsive genes. *Mech. Dev.* **80**, 171–180 (1999).
41. Knust, E., Schrons, H., Grawe, F. & Campos-Ortega, J. A. Seven genes of the Enhancer of split complex of Drosophila melanogaster encode helix-loop-helix proteins. *Genetics* **132**, 505–518 (1992).
42. Delidakis, C. & Artavanis-Tsakonas, S. The enhancer of split [E(spl)] locus of Drosophila encodes seven independent helix-loop-helix proteins. *Proc. Natl. Acad. Sci. U. S. A.* **89**, 8731–8735 (1992).
43. Baker, N. E. & Brown, N. L. All in the family: Proneural bHLH genes and neuronal diversity. *Dev.* **145**, (2018).
44. Alifragis, P., Poortinga, G., Parkhurst, S. M. & Delidakis, C. A network of interacting transcriptional regulators involved in Drosophila neural fate specification revealed by the yeast two-hybrid system. *Proc. Natl. Acad. Sci. U. S. A.* **94**, 13099–13104 (1997).
45. Giagtoglou, N., Alifragis, P., Koumbanakis, K. A. & Delidakis, C. Two modes of recruitment of E(spl) repressors onto target genes. *Development* **130**, 259–270 (2003).
46. Giagtoglou, N., Koumbanakis, K. A., Fullard, J., Zarifi, I. & Delidakis, C. Role of the Sc C terminus in transcriptional activation and E(spl) repressor recruitment. *J. Biol. Chem.* **280**, 1299–1305 (2005).
47. Jiménez, F. & Campos-Ortega, J. A. Defective neuroblast commitment in mutants of the achaete-scute complex and adjacent genes of D. melanogaster. *Neuron* **5**, 81–89 (1990).
48. Bier, E., Vaessin, H., Younger-Shepherd, S., Lily Yeh Jan & Yuh Nung Jan. deadpan, an essential pan-neural gene in Drosophila, encodes a helix-loop-helix protein similar to the hairy gene product. *Genes Dev.* **6**, 2137–2151 (1992).
49. Caudy, M. *et al.* The maternal sex determination gene daughterless has zygotic activity necessary for the formation of peripheral neurons in Drosophila. *Genes Dev.* **2**, 843–852 (1988).
50. Brand, M. & Campos-Ortega, J. A. Two groups of interrelated genes regulate early neurogenesis in Drosophila melanogaster. *Roux's Arch. Dev. Biol.* **197**, 457–470 (1988).
51. Schmidt, D. *et al.* ChIP-seq: Using high-throughput sequencing to discover protein-DNA interactions. *Methods* **48**, 240–248 (2009).

52. Zhang, Y. *et al.* Model-based analysis of ChIP-Seq (MACS). *Genome Biol.* **9**, (2008).
53. Yu, F., Kuo, C. T. & Jan, Y. N. Drosophila Neuroblast Asymmetric Cell Division: Recent Advances and Implications for Stem Cell Biology. *Neuron* **51**, 13–20 (2006).
54. Zhu, S. *et al.* The bHLH Repressor Deadpan Regulates the Self-renewal and Specification of Drosophila Larval Neural Stem Cells Independently of Notch. *PLoS One* **7**, (2012).
55. Zacharioudaki, E., Magadi, S. S. & Delidakis, C. bHLH-O proteins are crucial for Drosophila neuroblast self-renewal and mediate notch-induced overproliferation. *Development* **139**, 1258–1269 (2012).